# SITE DIRECTED MUTAGENESIS OF SEVERE ACUTE RESPIRATORY SYNDROME (SARS) CORONAVIRUS NSP 15 ENDORIBONUCLEASE

A Senior Honors Thesis

by

K. Maravet Baig

Submitted to the Office of Honors Programs
& Academic Scholarships
Texas A&M University
in partial fulfillment of the requirements of the

UNIVERSITY UNDERGRADUATE
RESEARCH FELLOWS

April 2006

Major: Molecular and Cell Biology and Biomedical Science

# SITE DIRECTED MUTAGENESIS OF SEVERE ACUTE RESPIRATORY SYNDROME (SARS) CORONAVIRUS NSP 15 ENDORIBONUCLEASE

A Senior Honors Thesis

by

K. Maravet Baig

Submitted to the Office of Honors Programs
& Academic Scholarships
Texas A&M University
in partial fulfillment of the requirements of the

UNIVERSITY UNDERGRADUATE
RESEARCH FELLOWS

Approved as to style and content by:

| | |
|---|---|
| --- | --- |
| Linda A. Guarino | Edward A. Funkhouser |
| (Fellows Advisor) | (Executive Director) |

April 2006

Major: Molecular and Cell Biology and Biomedical Science

# ABSTRACT

Site Directed Mutagenesis of Severe Acute Respiratory Syndrome (SARS) Cornavirus Nsp 15 Endoribonuclease (April 2006)

K. Maravet Baig
Department of Biology
Texas A&M University

Fellows Advisor: Dr. Linda A Guarino
Department of Biology, Biochemistry, and Entomology

In 2002-2003 SARS Coronavirus (SARS- CoV) spread throughout the world resulting in a 10% death rate. With little known about SARS-CoV, research must be done in order to understand the viral mechanism for structure based drug design in the future. The purpose of this research is addition to the current body of knowledge concerning SARS-CoV proteins, especially that of the Nsp15 endoribonuclease and its activity.

Nsp15 is a non-structural protein of SARS-CoV with endoribonuclease activity. Nsp15 recognizes and cleaves at uracil with a $Mn^{2+}$ cofactor; (Endoribonucleases cut in the interior of RNA strands). It was hypothesized that the uracil recognition may be indicated by four conserved asparagine residues. To test this, one of the conserved asparagine residues was mutated for analysis.

Site directed mutagenesis of Nsp15 with a QuickChange kit was performed. The $4^{th}$ asparagine, N, was mutated to alanine in one sample and to serine in another sample, making N4A and N4S mutants respectively. The $4^{th}$ amino acid was chosen due to the

flanking amino acid's known ability to affect activity. Nsp15 forms a hexamer, if the mutation caused the hexamer conformation to be disrupted, activity would be affected.

N4A and N4S mutant proteins were created, and their catalytic activities were tested. N4F, another mutant protein was tested, where phenylalanine replaced asparagine in the $4^{th}$ amino acid position. Dilutions of the three mutants were tested in order to compare the mutant activity with the wild type Nsp15 activity. N4S and N4A showed activity, but the N4F mutant did not.

Since N4F had no activity, it was inferred that the mutation caused a conformational change in the protein thereby affecting activity. Since hexamerization is protein concentration dependent, different concentrations should be tested in order to find out if the protein is active at higher concentration, or if it forms hexamers. A determination of the binding affinity of the mutant Nsp 15 for the known co-factor $Mn^{2+}$ should also be conducted as well as the examination of conformational changes brought about by addition of $Mn^{2+}$. Lastly, failure to bind the RNA substrate may cause inactivity; this possibility should also be tested.

# DEDICATION

I would like to dedicate this thesis to my beloved grandmother Dr. Ayesha Baig, MD. She has been an inspiration to me, and to all who know her. She was a physician and a scientist in a time when women were rarely seen in the medical profession. Thank you for all that you have done in science, in medicine, and in our family. I love you.

# ACKNOWLEDGEMENTS

I would like to thank many people in this endeavor. First of all I would like to thank God for allowing me to have this amazing opportunity. I would also like to whole heartedly thank Dr. Guarino for her time, amazing knowledge, and support. I would also like to thank Michele Balihe, Wen Dong, and Lillian Li for being there for my incessant questions. You were patient, kind, and a joy to be around. Thank you all.

I would like to thank my parents, M.K. and Connie Baig for their love, and their support. I would also like to thank my good friend Jessica Mackey, who helped me through the stressful times of research and writing the thesis. Thank you for your friendship. I would like to thank Madeline Louise; thank you for being you. Finally, I would like to thank the Office of Honors Programs and Academic Scholarships for partial research funding.

# TABLE OF CONTENTS

Page

# LIST OF FIGURES

# LIST OF TABLES

# INTRODUCTION

## SARS-CoV the Causative Agent of SARS

Coronaviruses are pathogens known to cause respiratory disease in humans (15). The Severe Acute Respiratory Syndrome (SARS) Coronavirus spread throughout China, Canada, and 30 other countries in the winter of 2002-2003. A death rate of 10% was estimated from the 8,000 known cases (28, 31); this mortality rate was staggering to the scientific community. Until the SARS outbreak, the known human coronaviruses caused "cold-like" symptoms, and were not usually life threatening. Within animal populations, especially that of avians and felines, coronavirus infection is much more severe; in retrospect, the human mortality rate probably should not have been unanticipated. SARS was first hypothesized to be a mutant strain of a pre-existing coronavirus, however, DNA sequence analysis proved this theory wrong showing that SARS was, in fact, a novel coronavirus. In April of 2003, the CDC (Centers for Disease Control and Prevention) announced that the full-length genetic sequencing of the genome of the SARS-associated coronavirus (SARS Co-V) had been completed (20).

---

This thesis follows the format of the *Journal of Virology*.

A coronavirus isolate similar to the SARS-CoV genome was found in civet cats of the exotic meat markets in China. This information suggested that SARS had "jumped species" (Zoonotic transfer) from animals to humans, as was the case for HIV, West Nile, and other recently emerged viruses (22).

SARS-CoV as Compared with Other Coronaviruses

SARS coronavirus shares many characteristics with other members of the coronavirus family. SARS-CoV particles are irregularly-shaped, with club-shaped peplomers extending from the outer envelope. The peplomers give the virus a crown-like appearance, thus the Latin word corona, meaning crown. The SARS-CoV genome also has similarities and differences with other coronaviruses. Many positive-stranded RNA viruses, such as SARS-CoV, produce a single polyprotein or either separate non-structural and structural precursor polypeptides that are cleaved by virus-encoded or host-encoded proteinases to render functional subunits (6).

The SARS RNA genome (32 kb) has a 5' cap, and a 3' poly (A) tail. Proteins for viral RNA synthesis are encoded at the 5' end of the SARS-CoV genome; four viral structural protein genes, S, M, E, and N; and several (around eight) presumed accessory genes. This characteristic is retained throughout coronaviruses (14, 26, 29). Although eukaryotic RNAs are usually monocistronic, it was discovered that 27 different genes were coded for in a single RNA. This was explained by the synthesis of several subgenomic RNAs and by proteolytic cleavage of two large polyproteins encoded by the virus. Both of these processes are unique to the virus and, therefore, represent potential targets for antiviral activity. (26, 29, 3, 14)

One potential target for research is non-structural protein 15 (Nsp 15), which has been shown to be an endoribonuclease that uses $Mn^{2+}$ as a cofactor (3). To better understand the mechanism of Nsp15 function and its role in viral replication, a set of site-directed mutant versions of Nsp15 will be constructed. These mutant proteins will be purified and tested for biological activity. The information gained from this study will be useful in future attempts to identify enzyme inhibitors that could potentially control virus replication.

Objective of this Research Endeavor

Drug treatment of SARS during the epidemic was largely ineffective. Previous efforts to develop vaccines for avian and feline coronaviruses have also proven unsuccessful, probably due to the presence of many different strains of coronaviruses coupled with their high rate of mutation. For this reason, research in the area of structure-based drug design offers the most promising hope in controlling future outbreaks.

Anti-viral medication for the treatment of SARS-CoV must be highly specific in order to inhibit the enzymatic activity of the viral Nsp 15 endoribonuclease, but not inhibit similar host cells proteins. With the high level of specificity required, inquiries must be made concerning the processes that are unique to the virus, and not commonly shared by the host cell. Research concerning Nsp 15 endoribonuclease has lead to better understanding of the viral machinery, and more specifically the structure and activity of Nsp 15, which is the primary target for manipulation.

The goal of this research concerned Nsp15 and its potential role in synthesis of subgenomic RNAs. Nsp 15, an endoribonuclease that cleaves on the 5' end of uridylates

could potentially be involved in this process. The goal was to conduct a structure/function analysis of Nsp 15 endoribonuclease in order to define residues that are essential for activity. Site directed mutagenesis was conducted in order to make mutant versions of Nsp 15 endoribonuclease. The mutant proteins were analyzed to determine the effect of the amino acid substitutions on the catalytic activity. One mutant was found to have no activity. With this result, future research should include Nsp 15 inquires regarding $Mn^{2+}$ binding, RNA binding, and conformational effects on Nsp15 brought about by the mutation.

# CHAPTER I

# LITERATURE REVIEW

## A Brief History of SARS Coronavirus

Severe acute respiratory syndrome coronavirus (SARS-CoV) was first discovered in Guangdong Province, China in the fall of 2002. In February 2003, after failed attempts to control the virus, the World Health Organization (WHO) was alerted of the crises. In this same month, the general public became aware of the virus after a woman from Hong Kong died while visiting her family in Toronto, thereby spreading the virus to North America. The eventual spread of the virus to 30 countries catalyzed a worldwide effort to discover the cause of SARS, and how it could be controlled. It was discovered that SARS-CoV was not simply a mutant of a pre-existing coronavirus, but was a novel coronavirus with a possible Zoonotic origin (2).

Although most evidence for species jump has labeled the civet cat as the Zoonotic agent, recent research suggests that the civet may have merely served as a source of viral magnification. Sequence analysis of SARS-CoV obtained from Chinese Horseshoe bats showed that the Chinese Horseshoe bats may have been the origin of the novel coronaviral strain (16). The fairly recent Zoonotic jump may be a result of the instability of the SARS -CoV genome. Evidence suggests that the mutation rate of the SARS-CoV genome, along with several open reading frames (ORFs) may play a role in the virulence of SARS-CoV as well as contribute to the possibility of a SARS epidemic anywhere in the world (10, 13).

Research continues on SARS in order to better understand the viral mechanism and structure so that anti-viral treatments, as well as better ways of containment may be designed. The following provides a brief review of recent SARS-CoV publications as pertinent to Nsp 15 endoribonuclease research.

Newly Discovered Way of SARS-CoV Transmission

In 2005, Wang et al. (30) conducted research on the detection of SARS coronavirus in human excrement from Xiao Tang Shan Hospital and the 309th Hospital of the Chinese People's Liberation Army. Through Wang's research, it was revealed that SARS-CoV could be spread through the feces of those infected with the virus. Electropositive filter media particle was used in order to concentrate the SARS-CoV taken from the sewage of two hospitals in Beijing with SARS patients. Cell culture along with semi-nested RT-PCR, and gene sequencing was used to verify the SARS-CoV RNA in the sewage. No live SARS-CoV was detected in the previously mentioned assays, but it was found that the coronavirus has the ability to survive at 4 ºC for 14 days and at 2 º C for 2 days. With these findings, it is now know that the excrement of SARS-CoV patients must be handled and disposed of with great care (30). With the possibility that SARS-CoV could still be spread today even in human excrement, more insight to the proteins coded for by the virus is necessary.

The Immunology of Infection with SARS-CoV

Zhang et al (33) proposed that patients with SARS-CoV who recovered from or died as a result of the virus were thought to have different neutralizing antibody (Nab) responses. Temporal changes in S glycoprotein-specific neutralizing antibody (Nab) and N protein-specific antibodies were analyzed. The patients that survived SARS-CoV infection had higher and prolonged levels of N protein-specific and S glycoprotein-

specific Nab responses (33). This suggested the probability of antibody responses in determining the definitive disease outcome of SARS-CoV patients (33).

SARS-CoV Proteins and Their Role in Immunity

SARS-CoV codes for both structural and non-structural proteins. Buchholz et al (4) explored the importance of the structural proteins by expressing them in parainfluenza virus (PIV) type 3 vector BHPIV3. Since SARS-CoV is a respiratory virus, this influenza vector provided immunization of the major sites of SARS-CoV transmission, also common in influenza. One of the structural proteins investigated was S (spike) glycoprotein. It was found that vaccination with BHPIV3 expressing S offered total protection against SARS-CoV in the lower respiratory tract, and partial protection in the upper respiratory tract. These results imply that S glycoprotein may act as the best neutralizing antigen of SARS-CoV (4).

Structural Proteins and Structural Analysis of SARS-CoV

Structural proteins have also been investigated for a better understanding of SARS-CoV and possible drug design. In December 2005, Bartlam et al. researched the configuration of SARS-CoV structural proteins (1). As mentioned earlier, the RNA genome of SARS-CoV encodes eight accessory proteins, four structural proteins, and sixteen non-structural proteins. As the structure of SARS-CoV macromolecules are elucidated, functions of the virus such as replication, transcription, and the fusion of viral and host membranes can be better comprehended. The main protease and spike protein (structural) fusion core have been studied at length with the endeavor of creating therapeutics against SARS-CoV (1, 12, 8). The structures and functions of most SARS

proteins remain unknown necessitating further study on their structure, as well as the ultrastructure of SARS-CoV (1).

The surface ultrastructure of SARS-CoV was explored with atomic force microscopy. (18) This research was the first direct scale nanometer characterization of the surface ultrastructures of SARS-CoV particles. The virion was directly visualized; dimensions for the structural proteins were provided with quantitative measurements. After treatment with hydroxyoctanoic acid, the corona, or crown like, appearance of large protrusions in the envelope were measured (18). The surface of each single SARS-CoV was surrounded with at least 15 spherical spikes having a diameter of 7.29 +/- 0.73 nm as seen with high-resolution images. This is in agreement with that of S glycoprotein which was predicted earlier using the genomes of SARS-CoV (18). Using the S glycoprotein prediction, Zhang et al. hypothesized that the disease outcome of individuals infected with SARS-CoV was correlated with the antibody response against SARS-CoV.

Site Directed Mutagenesis and Structural Protein Function

Spike (S) glycoprotein, a SARS viral envelope component, has the ability to induce an immune response. Research on the importance of S glycoprotein and the receptor, angiotensin converting enzyme II (ACE II) has been conducted, and has proven promising in the area of drug design. (32) Neutralizing antibodies, (NAbs) against SARS-CoV S glycoprotein has experimentally been shown to be protective in animals infected with the pseudo-viral pathogen. Empirical research suggests a possible way to stop the viral mechanism by interfering with the ligand (S glycoprotein) binding to the receptor (ACE II) (32).

Pseudovirus-based assays were used to evaluate the impact of viral entry and immunogenicity; the binding cleft in the S glycoprotein was evaluated, and 8 basic amino

acids were removed by site directed mutagenesis, and replaced with alanine. With this removal, it was found that mice vaccinated via DNA failed to produce NAbs. Point mutations were made in the amino acid sequence with varying results. R441A stopped viral entry as well as immune response; however, R453A only prevented viral entry (32). The site directed mutagenesis assay can be used with other nonstructural proteins of SARS-CoV in order to bring about changes in the activity of the protein via structural changes.

Catalytic Site of a SARS-CoV Structural Protein

Cinanserin, serotonin antagonist, has been found to inhibit the SARS-CoV 3C-like proteinase ($3CL^{pro}$). Because $3CL^{pro}$ is fundamental to the viral life cycle, it may be one of the best known targets for structure based drug design. Chen et al. studied a large data base of drugs in order to compare structural information of the existing drugs with that of crystallographic structure of the binding region of $3CL^{pro}$. After treatment with Cinaserin, it was found that the activity was decreased, and in tissue samples inhibition was seen. Though this drug may inhibit $3CL^{pro,}$ better proteins for inhibition may be found (5). Because of the high mutation rate of the SARS-CoV proteins, more information needs to be obtained on all SARS-CoV proteins, such as the nonstructural proteins, for structure based drug design to be an effective treatment.

SARS-CoV Nonstructural Proteins

The SARS-CoV RNA genome encodes proteins essential for genome replication and RNA transcription. These proteins are encoded as large polyproteins which are eventually proteolytically processed by virus-encoded proteinases producing mature replicases. Antibodies against SARS-CoV proteins were generated against predicted

replicase proteins. Antibodies were used to identify and characterize Nsp1, Nsp2, Nsp3, Nsp4, Nsp5, Nsp8, Nsp9, Nsp12, Nsp13, Nsp14, Nsp15, and Nsp16. These 12 proteins were predicted to be mature replicase proteins in SARS-CoV-infected Vero cells. Immunoblot analysis was used to predict protein sizes. 6 hours post-infection similar patterns of "punctate perinuclear" and distributed "cytoplasmic foci" with all replicase antibodies were detected using immunofluorescence microscopy. Co-localizations of replicase protein Nsp8 with Nsp3 and Nsp2 in cytoplasmic complexes were determined with "dual-labeling" studies (23).

Assay of SARS-CoV Nonstructural Proteins

Similarities between Murine Hepatitis Virus (MHV) and SARS have given researchers a venue to obtain more information on SARS-CoV and its associated proteins. In this study, SARS-CoV nucleocapsid and Nsp 12 were detected through anti-MHV virions and RNA-dependent RNA polymerase. The results from this study confirmed the hypothesized processing pattern for mature SARS-CoV replicase proteins. The findings suggested conservation of protein epitopes in the replicase and nucleocapsid of SARS-CoV as well as group II coronavirus, MHV (23, 27). Research results also indicate ability of replicase antibodies to detect SARS-CoV-infected cells as early as 6 hours post infection; this information adds to the body of literature used for studies of SARS-CoV inhibition, replication, and diagnosis. Independent labs continue to research the individual proteins of SARS-CoV, such as Nsp 12. (23)

ORFs Yield More Information on SARS-CoV Nonstructural Proteins

RNA codes for various open reading frames (ORFs) that may ultimately be transcribed into protein (24, 34). SARS- CoV has several open reading frames; the positive stranded RNA genome of SARS–CoV encodes ORF1 (9, 7). Of the nonstructural proteins, Nsp 1 and Nsp2 have been found to contain the most variable sequences, while the other 14 nonstructural proteins seem to be more conserved. Deletions in the coding sequence of Nsp 2 were performed in order to determine the importance of Nsp 2 in viral replication. As result of the deletion, the viral growth and RNA synthesis were slowed. Resulting from this research by Graham et al, a better method for the determination of other nonstructural proteins, such as Nsp 9 or Nsp 15, was established by using reverse genetic systems (9, 7).

Functions of Nonstructural Proteins in Greater Detail

It was hypothesized by Li et al. that the interaction of Nsp 10 with the cellular oxido-reductase system would cause extensive cytopathic effect (17). To test this idea, yeast two hybrid assay was used to screen for proteins that interacted with Nsp 10 in the cDNA library of a human embryo lung (17). As indicated by the results, apart from BTF3 and ATF5, two subunits of cellular RNA polymerase, Nsp10 also interacted specifically with the NADH 4L subunit and cytochrome oxidase II (17). A change in the activity of the NADH-cytochrome as well as depolarization of the inner mitochondrial matrix was found as a result of the Nsp10 protein gene in the transfected lung fibroblast. This result indicates one possible viral mechanism used by SARS-CoV in infection (17).

Previous SARS-CoV Nsp 15 Studies

Bhardwaj et al. (3) showed that SARS-CoV Nsp15 protein was a ribonuclease that cleaved 5' uridylates in RNA substrates. Through experimental results, manganese was found to be the preferred cofactor (3). Moreover, if the 5' or 3' terminus was blocked, the cleavage pattern remained unchanged indicating that it was an endoribonuclease. Both Double- and single-stranded RNAs acted as substrates for the endoribonuclease, although kinetics were faster for single-stranded RNA indicating that it was the preferred substrate. $Mn^{2+}$ was found to act as a co-factor, and was necessary for the best enzyme activity. Other divalent metals, such as $Mg^{2+}$, were tested, but produced less endoribonuclease activity. Contingent to the level of endoribonuclease activity of Nsp 15 was the concentration of $Mn^{2+}$. Using Tryptophan fluorescence, $Mn^{2+}$ was shown to induce conformational changes in the protein in a concentration-dependent manner. An orthologous protein of another coronavirus was tested, and found to display endoribonuclease activity. It was hypothesized that Nsp 15 endoribonuclease is common to the coronavirus family (3).

Nsp 15 Research Influence by another RNase

Numata et al (21) showed that substrate specificity of a different uridine-specific RNase in the RNase T2 family could be changed from uridine to guanine by mutation of asparagine 71 to serine or threonine. With this change in specificity, more information was obtained about the active site, and substrate binding. (21) Given the similarity of the RNA substrates and uridylate specificity of T2 RNase, to Nsp 15 endoribonuclease, it was hypothesized that similar mutations in Nsp 15 may render information about the catalytic sites of Nsp 15, as well as its activity. In Nsp 15, the fourth amino acid,

asparagine, was mutated to serine (N4S) and alanine (N4A) and the activity of the mutants were tested.

Why SARS-CoV Research is Important

Recurrence of SARS-CoV still poses a threat because the causative agent lingering in animal reservoirs is not wholly understood. Sporadic cases continue to be reported, and serve as a reminder that research on SARS-CoV must continue (19). With increasing knowledge of SARS-CoV and its proteins, better ways of treating the virus, and containing the virus should future outbreaks occur, will be possible.

# CHAPTER II

# MATERIALS AND METHODS

## Site Directed Mutagenesis

Oligonucleotides for N4A and N4S were ordered from Invitrogen™ with the desired mutations; the 4$^{th}$ amino acid, asparagine, N, was mutated to alanine, A, in one oligonucleotide and to serine, S in the other. In order to construct the N4A and N4S mutants, a QuikChange™ kit purchased from Stratagene© was employed; before usage, the kit was stored at -20°C as suggested by the manufacturer. The QuikChange™ kit provided Quik Solution™ used in the procedure (it was suggested to leave the Quick™ Solution off ice while preparing the samples due to its ability to quickly freeze). The kit also included 10X reaction buffer, a dNTP (deoxy-nucleotide triphosphate) mix, and a Pfu mix.

Quick Solution, 10X reaction buffer, dNTP mix, Pfu mix, along with mutagenic primers, template DNA, and $H_2O$ were added together making the mutagenesis reaction with a final volume of 50μL; the final volume of 50 μL was chosen arbitrarily. The solution per volume added can be seen in Table 2.1.

| | | | |
|---|---|---|---|
| 10X Reaction Buffer | 5 µL | dNTP mix | 1 µL |
| 10 ng/µL Template DNA (Nsp 15 WT) | 1 µL | *Quick Solution*© | 3 µL |
| 100ng/µL N4A (or N4S) primer 1 | 1.25 µL | Pfu mix (DNA polymerase) | 1 µL |
| 100ng/µL N4A (or N4S) primer 2 | 1.25 µL | $H_2O$ | 36.5 µL |

**Table 2.1**: Solution per volume added for mutagenesis protocol

The primers were obtained in a 1 µg/µL solution. Further dilutions had to be made in order to aliquot 100ng/µL primer solutions. Since 1µg/µL is equivalent to 1000 ng/µL a 1:10 dilution was performed; 1 µL of primer + 9 µL of $H_2O$ for 10 µL, or, 2 µL of primer + 18 µL of $H_2O$ for 20 µL. The larger volume was used. The template DNA (Nsp 15 WT) was available in a 3.05 ng/µL solution. (It should be noted that the procedures as described were performed for both N4A and N4S.)

In order to obtain the desired 10 ng/μL, it was observed that 3.05 ng/μL was the same as 3050 μg/μL. A total volume of 500 μL was arbitrarily chosen due to convenience; 1.6 μL of DNA was calculated and added to 498.8 μL of $H_2O$ which yielded the desired concentration of 10 ng/μL of template DNA. Once the entire mutagenesis solution was prepared, as seen in Table 2.1, the sample was transported on ice to the Eppendorf Mastercycler PCR for Polymerase Chain Reaction, which amplified the plasmid containing Nsp 15 and incorporated the desired mutations.

The mutagenesis PCR consisted of 20 cycles which served to melt the DNA, anneal the primers, and finally elongate the DNA with the desired mutations. First, the mutagenesis sample was held at 95°C for 1 min, followed by 18 cycles of 95°C for 50 sec, 55°C for 50 sec, and 68°C for 6 min. The final cycle was 68°C for 6 min. After PCR, the mutagenesis sample was removed from the Eppendorf Mastercycler PCR and placed on ice for a few seconds (see Figure 2.1 for thermocycler machine).


**Figure 2.1**: Picture of thermocycler machine

Transformation into XL-10 Gold Competent Cells

One µL of the restriction enzyme Dpn I was added to the sample in order to digest the parental DNA strand, leaving only the newly replicated DNA. (Dpn I was used as a consequence of the methylated guanine; cleavage using DpnI is between A and T.) The treated sample was put in a 37 °C water bath for 1 hour. The XL-10 Gold Cells (competent cells) for transformation were removed from the -80°C freezer and were allowed to melt while on wet ice. After the competent cells had liquefied, 2µL of β-Mercaptoethanol was added to the cells.

The mixture was left on ice for 10 minutes. 3 µL of each mutagenesis reaction was pipetted into the competent cells. The cells were not mixed by pipetting up and down; the tube was flicked in order to carefully mix without damaging the cells. The sample was then incubated on ice for 30 minutes. After this, the sample was heat-shocked for precisely 30 seconds by placing the mixture in a 42ºC water bath. The sample was not shaken. Upon removal from the water bath, the sample was placed on ice for 2 minutes. 900 µL of pre-warmed SOB media was added. Following this addition, the sample was taped on its side in a shaking incubator and allowed to shake at 225 rpm for 1 hour at 37ºC. After shaking, 100 µL, 150 µL, and 250 µL of the transformation were spread, while near an open flame, on to 2 separate LB agar plates with ampicillin. The residual transformation reaction mixture was stored at 4 ºC overnight. The spread LB-$Amp^+$ plates were placed upside down and incubated overnight at 37ºC to allow colonies to grow.

Purification of Mutant DNA

A well isolated colony (see Figure 2.2) was picked from the LB-$Amp^+$ plate with the end of a sterile wooden pick; this was also performed near an open flame. The colony was then placed into 5 mL of LB medium with ampicillin. The culture was then allowed to shake at 300 rpm overnight at 37 ºC. After the required time had elapsed, the bacterial cells were harvested at 6000 rpm for 15 minutes at 4 ºC in a Beckman Model J2-21 centrifuge using a JA-14 rotor. The bacterial pellet formed during centrifugation was resuspended in 4 mL of Buffer P1 (provided in the Qiagen© plasmid kit). The P1 buffer contained RNase A, and to ensure the bacteria were completely resuspended, the sample was pipetted up and down. After complete resuspension, 4 mL of Buffer P2 was added to

the sample. The sample tube was inverted 5 times to mix, and was incubated at room temperature for 5 minutes. 4 mL of chilled Buffer P3 was added to the sample, and immediately inverted 5 times. The sample was then incubated on ice for 20 minutes.

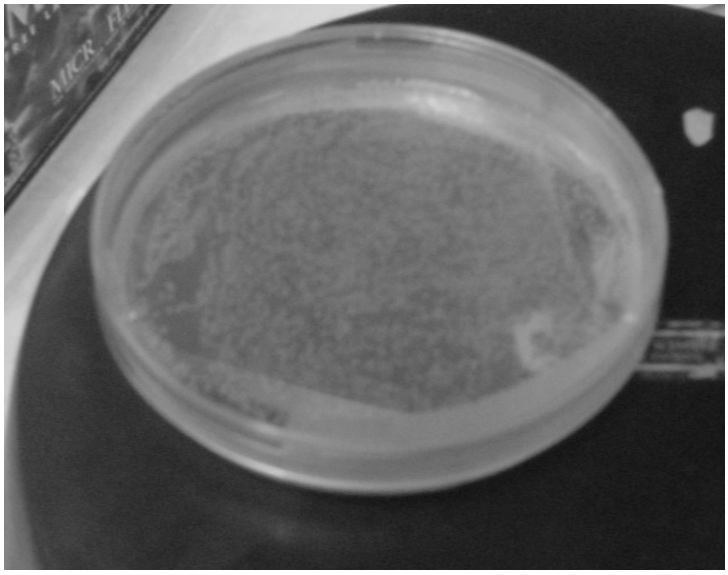

**Figure 2.2**: Example of colonies in LB-ampicillin plate

After incubation, the sample was centrifuged at 20,000 rpm at 4 ºC for 30 minutes. The supernatant contained the desired plasmid DNA, and was removed. The supernatant was centrifuged again at 20,000 rpm at 4 ºC for 15 minutes. The supernatant was removed promptly. 240 µL (collection 1) of the now cleared supernatant was removed for later use on an analytical gel. The QIAGEN-tip 100 was equilibrated by applying 4 mL Buffer QBT. The column was allowed to empty by gravity filtration. The

tip was completely drained before the successive step was performed. The supernatant was then loaded onto the QIAGEN-tip 100 and entered the resin by the force of gravity. 240 µL (collection 2) of the flow through was saved for analytical purposes. The QIAGEN-tip 100 was washed with 2 x 10 mL Buffer QC. 240 µL (collection 3) of the wash fractions were removed for analytical purposes. After this, the DNA was eluted with 5 mL of Buffer QF. 100 µL (collection 4) of the elution was saved for analytical purposes. 3.5 mL of room-temperature isopropanol was added to the elution to precipitate out the DNA. After this addition, the sample was immediately mixed, followed by centrifugation at 3750 rpm at 4 ºC for 60 minutes. Henceforward, the supernatant was poured off.

The DNA pellet form from the centrifugation was washed with 2 mL of room-temperature 70% ethanol. The supernatant was carefully poured off; the DNA pellet remained stuck to the side of the tube. The pellet was then air dried for 10 minutes. The DNA pellet was then re-dissolved in adequate volume of pH 8.0 TE buffer. Collections 1-4 were saved overnight at -20 ºC as well as the final purified DNA

Throughout the course of the max prep assay, care was taken not to shear the genomic DNA; because of this, the buffers were not mixed by vortex. To minimize salt precipitation with the purified DNA, the buffers were kept at room temperature. The purified DNA pellet produced by the max prep was around 500 µg as suggested by the Qiagen™ protocol. Care was taken not to throw out the isopropanol pellet due to its loose attachment to the side of the tube, and clear appearance.

For the DNA agarose gel analysis, collections 1-4, purified DNA, and standard molecular weight marker were run; since N4A and N4S were both purified, there were 8

total collections. The DNA gel was run at 110 volts. Table 2.2 expresses the volumes used to run on the gel of the collections, loading dye, and $H_2O$.

| | Sample | Dye | $H_2O$ |
|---|---|---|---|
| Collections 1-4 | 18 μL | 2 μL | - |
| Purified DNA (N4A & N4S) | 10 μL | 2 μL | 8 μL |

**Table 2.2**: Loading volumes for analytical agarose gel

Optimum density readings of the DNA were taken. OD readings should be between 0.8-1. 1 mL of $H_2O$ was placed into a UV spectrophotometer cuvette to calibrate the spectrophotometer in the UV region. 5 μL was then added to the $H_2O$. The readings for both N4A and N4S were obtained, and were used in determining the amount of DNA to add for each PCR mixture.

Sequencing of Purified DNA

To confirm the correct DNA mutation had taken place, sequencing PCR was run. The promoter and terminator were diluted 4:36 respectively and were pipetted into

separate PCR tubes. The mutant DNA was added to the PCR tubes containing promoter and terminator along with Big Dye. All volumes added can be found in Table 2.3.

| | | | | |
|---|---|---|---|---|
| DNA | (N4A)<br>6 μL | (N4A)<br>6 μL | (N4S)<br>4 μL | (N4S)<br>4 μL |
| T7<br>promoter/terminator | (promoter)<br>2 μL | (terminator)<br>2 μL | (promoter)<br>2 μL | (terminator)<br>2 μL |
| Big Dye | 2 μL | 2 μL | 2 μL | 2 μL |

**Table 2.3**: Volumes added to PCR tubes for sequencing

$H_2O$ was added to each of the above mixtures to make a total volume of 20 μL for each tube. For N4A, 10 μL of $H_2O$ was added; for N4S, 12 μL of $H_2O$. The sequencing PCR cycle was run on the samples: 2 minutes at 94°C (1X) 94°C for 15 seconds, 55°C for15 seconds, 72°C for 1 minute, and 72°C for 2 minutes (30X). After this, all contents were transferred into 1.5 mL tubes, and 5 μL of EDTA (250 mM) was added. To this mixture, 60 μL of room temperature 100% ETOH was added. After this addition, the mixture was spun at full speed at 4 °C for 15 minutes on a centrifuge. The supernatant was discarded, and the pellet was washed with 100 μL of 70% ETOH. The pellet was allowed to dry and was sent for sequencing

Protein Expression Assay for N4A and N4S

One μL of the mutant DNA was pipetted into 1 mL of thawed Star (S) competent cells. The cells were then incubated on ice for 30 minutes. Following this, the cells were heat shocked in a 42°C water bath for 45 seconds. 0.5 mL of SOB media was added to the cells, and the cells were shook for 37°C for 1 hour. 100 μL of the cells were spread onto an LB agar plate with ampicillin. The plate was incubated at 37 °C overnight.

After overnight incubation, 5 mL LB media was pipetted into a 50 mL tube. 5 μL of ampicillin was added to the 50 mL tube. After this, 5 well isolated colonies were chosen from the plate and placed into the tube. This procedure was carried out beside an open flame. The culture was then placed in a shaker for 4 hours at 37 °C. The bacterial culture became cloudy. While the culture was shaking, 1 L of LB media was prepared. 25 g of LB was added to 1L MiliQ purified water in a 4 L flask. The LB was then autoclaved for 20 minutes on the liquid cycle, with no dry time. The entire 5 mL culture was transferred into 1 L of warmed media; 1 mL of 50 mg/mL Ampicillin was added. The 1 L culture was then placed in a 37 °C shaker for 4 hours. The OD (optimum density) of the DNA was tested after 4hours; the OD was done in the visible light region at 600 nm. The readings for both N4A and N4S were obtained. After OD had been reached, the culture was cooled at 4°C; 0.5 mL of IPTG was added after adequate cooling. The cooled culture was placed at 16°C in a shaker for 36 hours.

The culture was centrifuged at 5,000 rpm for 10 minutes using the JA-14 rotor; the supernatant was discarded. The pellet was resuspended in 20 mL Nsp Buffer (see Table 2.4).

| Desired Concentrations | Volumes used to attain desired amounts |
|---|---|
| 300 mM NaCl | 30 mL of 5 M NaCl |
| 50 mM Tris ( pH 7.9) | 25 ml 1 M Tris |
| 10 % Glycerol | 50 mL |
| 2 mM β- Mercaptoethanol* | 28 μL |

**Table 2.4**: Volumes for Nsp Buffer
*add fresh to 200 mL of NaCl, Tris, and Glycerol

$H_2O$ was added to make the final volume 500 mL for the entire Nsp Buffer. Only 200 mL of this volume was used; β-Mercaptoethanol was added to the 200 mL solution. 30 mg of Lysozyme was added to the resuspended sample; it was incubated on ice for 10 minutes. Following this, the sample was sonicated for 2 minutes at 4°C. The duty cycle was set to 50%, and the output control set to 4.5. 20 μL of the sonicated sample was saved for 10% PAGE gel analysis. The sample was then centrifuged at 16,000 rpm for 30 minutes, with a JA-20 rotor. 20 μL of the supernatant was saved for gel analysis. All remaining supernatant was

mixed onto a Talon nickel affinity column (after the column had been prepared; see Figure 2.3).

**Figure 2.3**: Talon Nickel affinity column

The Talon column was prepared by adding 2 mL Talon resin to the plastic column. This was followed by a 5 mL $H_2O$ wash, 2 mL MES wash, and finally a 3 mL Nsp Buffer wash. The resin was resuspended into 5 mL Nsp Buffer, and

transferred into 50 mL tube. The resin was centrifuged on a medium speed for 10 minutes. The supernatant was poured off but the pellet of resin was saved. The Talon resin + supernatant from the sample shook on ice for 20 minutes. This was poured on to the column and allowed to empty by gravity flow. 20 µL of the flow through was saved for gel analysis. The column was then washed with 20 mL of Nsp Buffer. 175 µL of 10 mM Imidazole was added to 15 mL of the Nsp Buffer; this mixture was used to wash the column. 20 µL of wash flow through was saved for gel analysis. 3 x 1 mL of Nsp Buffer + 625 µL 250 mM Imidazole was used as a second wash; 20 µL of each 1 mL elution was saved for gel analysis. Loading dye was added to the samples. The samples were placed on a hot plate for 3 minutes before loading into the 10% PAGE gel. The amount of protein sample and loading dye used can be found in Table 2.5.

| Extraction phase | DNA | Loading Dye (1X or 2X) |
|---|---|---|
| Total | 4 μL | 20 μL 1X |
| Load | 4 μL | 20 μL 1X |
| Flow Through | 4 μL | 20 μL 1X |
| Elute 1 | 10 μL | 10 μL 2X |
| Elute 2 | 10 μL | 10 μL 2X |

**TABLE 2.5**: Volumes loaded into 10% SDS PAGE gel

The volumes used for the 10% SDS PAGE gel can be found in Table 2.6.

| Protein Gel (10% SDS gel) | |
|---|---|
| 30% Acrylamide | 12 mL |
| $H_2O$ | 14.5 mL |
| 1.5M Tris (pH 8.8) | 8.96 mL |
| 10% SDS | 360 µL |
| 10% APS | 240 µL |
| TEMED | 24 µL |
| **Stacking Gel** | |
| 30% Acrylamide | 1.28 mL |
| 0.5M Tris (pH 6.8) | 2 mL |
| $H_2O$ | 4.56 mL |
| 10% SDS | 80 µL |
| 10% APS | 80 µL |
| TEMED | 8 µL |

**Table 2.6**: Volumes used for preparing the 10% SDS PAGE gel

Fast Protein Liquid Chromatography (FPLC) purification

Low salt and high salt wash buffers were made for calibration of the FPLC. Tris, NaCl, Glycerol, and β-Mercaptoethanol were added in quantities as described in Table 2.7. Water was also added to the buffers in order to make a total buffer stock of 500 mL for each. B-Mercaptoethanol was added fresh to aliquot of the stock buffer.

| Low Salt Buffer | |
|---|---|
| 50 mM Tris ( pH 7.9) | 25 mL |
| 100 mM NaCl | 10 mL |
| 5% Glycerol | 25 mL |
| $H_2O$ | 440 mL |
| 2 mM β-Mercaptoethanol* | 21 μL |
| **High Salt Buffer** | |
| 50 mM Tris | 25 mL |
| 1 M NaCl | 100mL |
| 5% Glycerol | 25 mL |
| $H_2O$ | 350 mL |
| B-Mercaptoethanol* | 14 μL |

**Table 2.7**: Low salt and high salt FPLC column buffers
*must add fresh

The FPLC was allowed to calibrate with the high and low salt buffers before the sample was prepared. After the calibration, the protein sample was diluted to a lower salt concentration, from 300mM to 100 mM. The remaining volume of elute 1 and elute 2 (1 mL each) that were not used in the 10% SDS PAGE gel were added together (2 mL). 4 mL of no NaCl buffer, containing .1 mM EDTA and 50 mM Tris was added to the elutions; 4 mL of 100 mM NaCl buffer (low salt buffer) was added to make the total volume 10 mL. The 10 mL sample was transferred into 2 mL tubes and micro-centrifuged at full speed for 10 minutes at 4°C. The samples from the tubes were recombined and injected into the port hole of the FPLC intake column. The FPLC collections 1 mL fractions every minute; the highest peak fractions were collected and run on 10% SDS gel.

The fractions corresponding with the large bands from the 10% SDS gel were combined and dialyzed. For the dialysis, the tubing was soaked in $H_2O$ for 30 minutes. After this, the fractions were carefully pipetted into the dialysis tubing. 150 mL of enzyme storage buffer (50mM Tris pH 7.9, 400 mM KCl, 0.1 mM EDTA, and 50% Glycerol) + 1mM DTT (added 150µL fresh) were added to a 200 mL flask with magnetic stir bar. The dialysis tubing with the fractions were placed in the tubing and allowed to stir at 4 °C for 5 hours. The samples were then removed and frozen at -20 °C.

Protein Concentration Assay

Bovine Serum Albumin (BSA) was used as the standard concentration, BSA= 1 µg/ µL. Increasing amounts of the samples were loaded onto a 10% SDS gel and compared to BSA as described in Table 2.8.

| DNA | 1 µL | 2 µL | 3 µL | 5 µL | 7 µL | 10 µL |
|---|---|---|---|---|---|---|
| Loading Dye (1Xor 2X) | (1X) 20 µL | (1X) 20 µL | (1X) 20 µL | (2X) 15 µL | (2X) 13 µL | (2x) 10 µL |

**Table 2.8**: DNA dilutions for concentration analysis

Activity Assay

Twenty two mL of 28% Acrylamide-urea gel, 100 µL of 10% APS and 20 µL of TEMED were poured for the samples of N4A and N4S along with a new sample N4F. The gel was pre-run for 30 minutes at 200 volts; 1X TBE buffer was used. The wells were washed of urea before the samples were loaded by pipetting out each well. The samples (N4A, N4S, and N4F) were diluted using enzyme storage buffer (50 mM Tris pH 7.9, 400 mM KCl, 0.1 mM EDTA, 50% Glycerol and 1 mM fresh DTT) according to their concentrations as determined by the concentration assay. A mix (see Table 2.9) with radioactive RNA was made, on ice, with the addition of the radioactive isotope, Phosphorous ($^{32}$P). The mix was added to the samples of varying concentrations. There were 9 total samples and 1 extra, giving 10 total samples. The radioactive mix was prepared behind a shield.

| | |
|---|---|
| 50 mM Tris | 81 μL |
| 100 mM KCl | 8.1 μL |
| 1 mM DTT | 1.62 μL |
| 5 mM $Mn^{2+}$ | 8.1 μL |
| RNAsin | 4.5 μL |
| TRS ($^{32}$P labeled RNA) | 18 μL |
| $H_2O$ | 40.7 μL |

**Table 2.9**: Volumes of radioactive mix and mutant protein

9 μL of the radioactive mix was added to 1 μL of each of the 9 samples (DNA + enzyme storage buffer). However, additional radioactive mix was not added to the samples already containing radioactive mix (see Table 2.10). The samples, after the radioactive mix addition, were incubated at 37°C for 1 hour. 10 μL of loading dye was added to each sample and heated for 3 minutes on a hot plate. The wells were washed, and the samples were loaded onto the 28% Acrylamide-Urea gel. The gel exposed to phosphoimage film overnight. Radioactive imaging was used to read the phosphoimage.

| Sample | DNA | Enzyme Storage Buffer (or Radioactive mix if noted) |
|---|---|---|
| **Wild Type** (1250 ng/ μL) | | |
| 142 ng | 1.1 μL [a] | 8.9 μL [b] |
| 71 ng | 5 μL [(a+b)] | 5 μL [c] |
| 35.5 ng | 5 μL [(a+b+c)] | 5 μL [d] |
| 17.75 ng | 5 μL [(a+b+c+d)] | 5 μL |
| **N4A** 83 ng/ μL | | |
| 142 ng | 1.7 μL | 8.3 μL (radioactive mix) |
| 71 ng | 8.6 μL [a] | 1.4 μL [b] |
| 35.5 ng | 5 μL [(a+b)] | 5 μL [c] |
| 17.75 ng | 5 μL [(a+b+c)] | 5 μL |
| **N4S** 71 ng/ μL | | |
| 142 ng | 2 μL | 8 μL (radioactive mix) |
| 71 ng | 1 μL | 9 μL (radioactive mix) |
| 35.5 ng | 5 μL [a] | 5 μL [b] |
| 17.75 ng | 5 μL [(a+b)] | 5 μL |
| **N4F** 400 ng/ μL | | |
| Table II-J continued | | |
| 142 ng | 3.6 μL [a] | 6.4 μL [b] |
| 71 ng | 5 μL [(a+b)] | 5 μL [c] |
| 35.5 ng | 5 μL [(a+b+c)] | 5 μL [d] |
| 17.75 ng | 5 μL [(a+b+c+d)] | 5 μL |

**Table 2.10**: Dilution series used for phosphoimage

Hexamer Formation of N4F Tested

FPLC was used in order to test the hexamer formation of the N4F mutant protein. The Superdex 200 column was implemented. The protein sample was injected into the loop with a 1mL syringe. Fractions were collected, and were analyzed by the FPLC program for hexamer and monomer formation.

Protein Expression Assay for N4F

Protein Expression for N4F, Fast Protein Liquid Chromatography (FPLC) purification, protein concentration assay, and the activity assay were carried out as they had been for N4A and N4S (see above). For the protein expression of N4F, instead of running two elutions as was done for N4A and N4S, 3 elutions were run. N4F was also run along side N4A, N4S, and wild type in a 10% SDS gel for concentration analysis. The volumes loaded into the 10% SDS gel are given in Table 2.11.

| | | |
|---|---|---|
| N4A | (DNA) 12.1 µL | (2X loading dye) 8 µL |
| N4S | (DNA) 14.0 µL | (2X loading dye) 6 µL |
| N4F | (DNA) 20 µL | (1X loading dye) 1 µL |
| WT | (DNA) 20 µL | (1X loading dye) 1 µL |
| BSA | DNA) 20 µL | (1X loading dye) 1 µL |

**Table 2.11**: Volumes added to 10% SDS gel for concentration analysis

Re-sequencing of N4S and N4S 1.43

Two concentrations of N4S (1.87ng/µL and 1.43ng/µL) were obtained and re-sequenced. 0.25 µg/µL of each sample were needed. To facilitate this, 1.8 µL of N4S 1.43 was added to 7.2 $H_2O$. 1.4 µL of N4S 1.87 was added to 8.6 µL of $H_2O$. 2 µL of each DNA in $H_2O$ was then added to 2 µL of T7 terminator, and 2 µL of Big Dye for a total of 6 µL. Sequencing PCR was run on the samples: 2 minutes at 94°C (1X) 94°C for 15 seconds, 55°C for15 seconds, 72°C for 1 minute, and 72°C for 2 minutes (30X). After the PCR, 14 µL of $H_2O$ was added, along with 5 µL of 125 mM EDTA and 60 µL of ETOH. This mixture was allowed to sit at room temperature for 15 minutes. After this, the sample was spun at top speed at 4°C in the microcentrifuge. The supernatant was discarded. 50 µL of 70% ETOH was added to wash the pellet, and was slowly extracted from the tube. The tube was spun for 4 seconds at 4°C in the microcentrifuge; any

remaining 70% ETOH was removed. The pellet was allowed to air dry, and was subsequently sent for analysis at Applied Biosystems for sequencing analysis.

# CHAPTER III
# RESULTS AND DISCUSSION

Nsp 15 Endoribonuclease

Mutant proteins allow researchers to isolate specific regions of the protein as well as study the implications the said mutation has on enzymatic activity. The amino acid sequence of the protein is known as the primary sequence. Changes to the primary sequence usually yield changes in the overall 3D confirmation of the protein, known as the tertiary structure. Since protein form (3D confirmation) and function are interrelated, a change in one leads to change in the other). In this way, mutations in the amino acid sequence would yield conformational changes.

Functions of the wild type (normal) Nsp 15 endoribonuclease include binding RNA, recognition of uracil (U), binding of $Mn^{2+}$ cofactor, and catalyzing hydrolysis of the RNA substrate. These functions are thought to be fostered by the 3D conformation of the wild type Nsp 15. Endoribonucleases cleave in the middle of Ribonucleic Acid (RNA) strands; Nsp 15 specifically cleaves at uracil (U). Nsp 15 contains 4 conserved asparagine residues; it was hypothesized that one of these residues may be important for substrate recognition. For Nsp 15, the substrate is RNA (3).

With mutations of the wild type Nsp 15, comparisons could be made to better understand the function of the wild type (WT) and analyze the structure-function relationship.

As discovered in previous studies, wild type Nsp 15 exists in a state of dynamic equilibrium between two different 3D conformations: hexamers (see Figure 3.1) and monomers (11). It has also been suggested that the hexamer confirmation yields endoribonuclease activity. To test if amino acid substitution would translate into impaired

hexamer formation, site directed mutagenesis was used to create mutants of Nsp 15 endoribonuclease and their endoribonuclease activities were subsequently tested. The focus of this research was the activity of the wild type Nsp 15 versus that of the mutants N4A, N4S, and N4F.

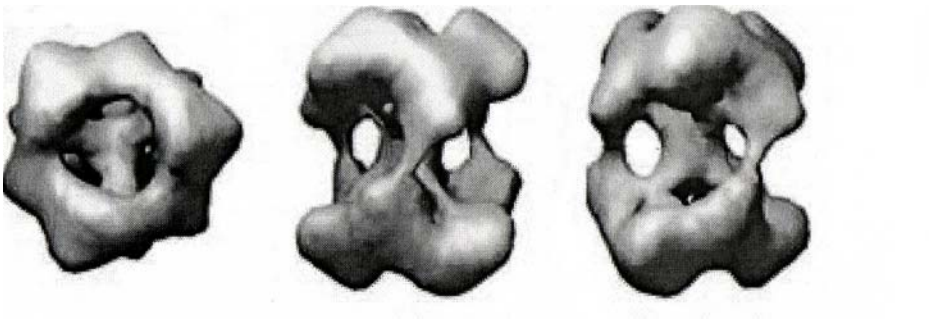

**Figure 3.1**: Hexamer confirmation of Nsp 15 endoribonuclease wild type. The different clefts are possible RNA binding sites. More information can be ascertained about the catalytic sites as more is discovered about the amino acid structure of the protein.

Analysis of Site Directed Mutagenesis

Site directed mutagenesis is an excellent way to study a protein's structural relationship to function. The QuikChange® kit implemented point mutations; the resulting protein had an amino acid change in one position only, thus the term point. Pfu mix was used due to its ability as polymerase to synthesize new pieces of DNA from a DNA template (24). For mutagenesis to take place Pfu replicates the plasmid, while leaving the mutated oligonucleotide primers in place; thus mutant DNA is created.

Oligonucleotides, also called primers, are short, single stranded pieces of DNA that can be used to insert into bacterial plasmids as seen in the QuikChange™ figure (see Figure 3.2); pET-15b was the vector used for Nsp 15. (Bacterial plasmids are double stranded (ds) circular DNA; pET-15b contained the promoter sequence for T7 RNA Polymerase.) The oligonucleotides have their nucleotide bases changed in such a way to ultimately yield a different DNA than the wild type DNA. Ultimately this will result in a mutated protein when it is synthesized from the mutant DNA. The oligonucleotides correspond to opposite strands of the plasmid, and allow inclusion into the plasmid by the polymerase Pfu.

The parent DNA (the template) was digested by an endonuclease, Dpn I. Dpn I is specific for 5′-Gm$^{6}$ATC-3′; the m refers to methylation. Bacterial DNA contains methylation on the Guanine (G); therefore the bacterial plasmids were digested, leaving the mutated DNA.

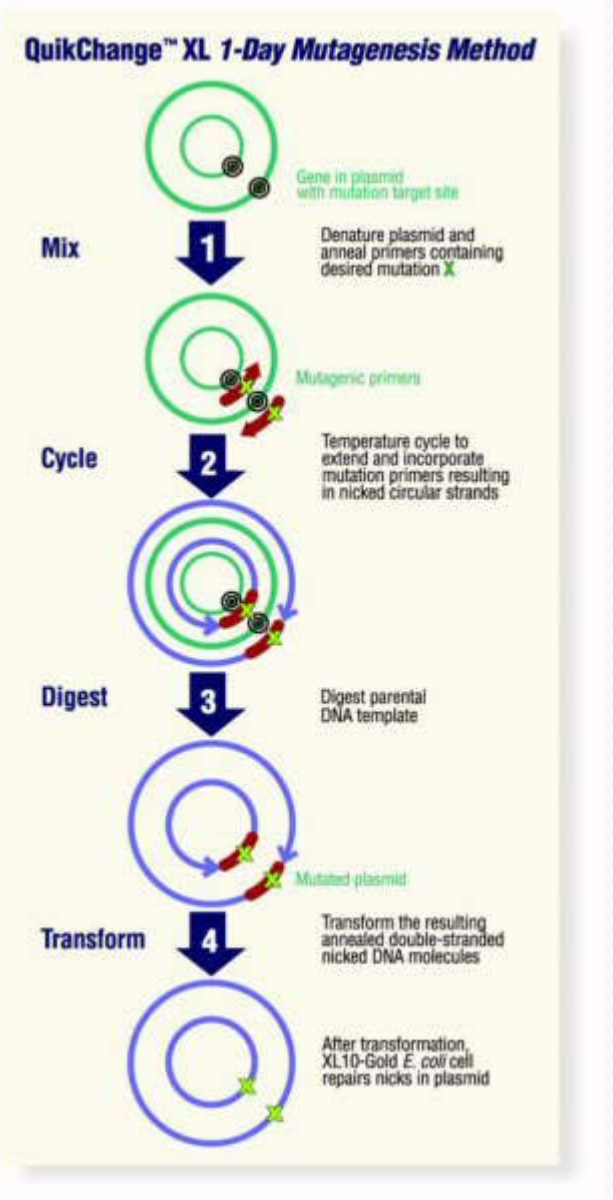


**Figure 3.2**: QuikChange™ Site-Directed Mutagenesis

DNA Concentration Results

The plasmid containing the desired mutations were transformed into XL-10 gold cells and grown in culture in Luria-Bertani (LB) medium with ampicillin for selection. Expression of Nsp15 in log-phase cells (Optimum density between 0.8 and 1.0) were

induced by the addition of IPTG allowing transcription of Nsp15 DNA. The DNA gel with purified N4A and N4S DNA can be seen in Figure 3.3.

**1** **6** **11**

**Figure 3.3**: DNA gel electrophoresis: 1$^{St}$ lane = molecular weight marker; 2$^{nd}$ -5$^{th}$ lanes = collections 1-4 N4A; 6$^{th}$ lane = purified N4A DNA; 6$^{th}$-10$^{th}$ lanes = collections 1-4 N4S; 11$^{th}$ lane = purified N4S

Sequencing PCR was run on the purified DNA to ensure the correct mutation had taken place. The purified DNA concentration for N4A and N4S were determined using UV spectroscopy. N4A was found to be 0.19µg/µL; N4S was found to be 0.26 µg/ µL. The purified DNA pellets were sent for analysis, as seen in the Electropherograms in Figure 3.4 for N4A.

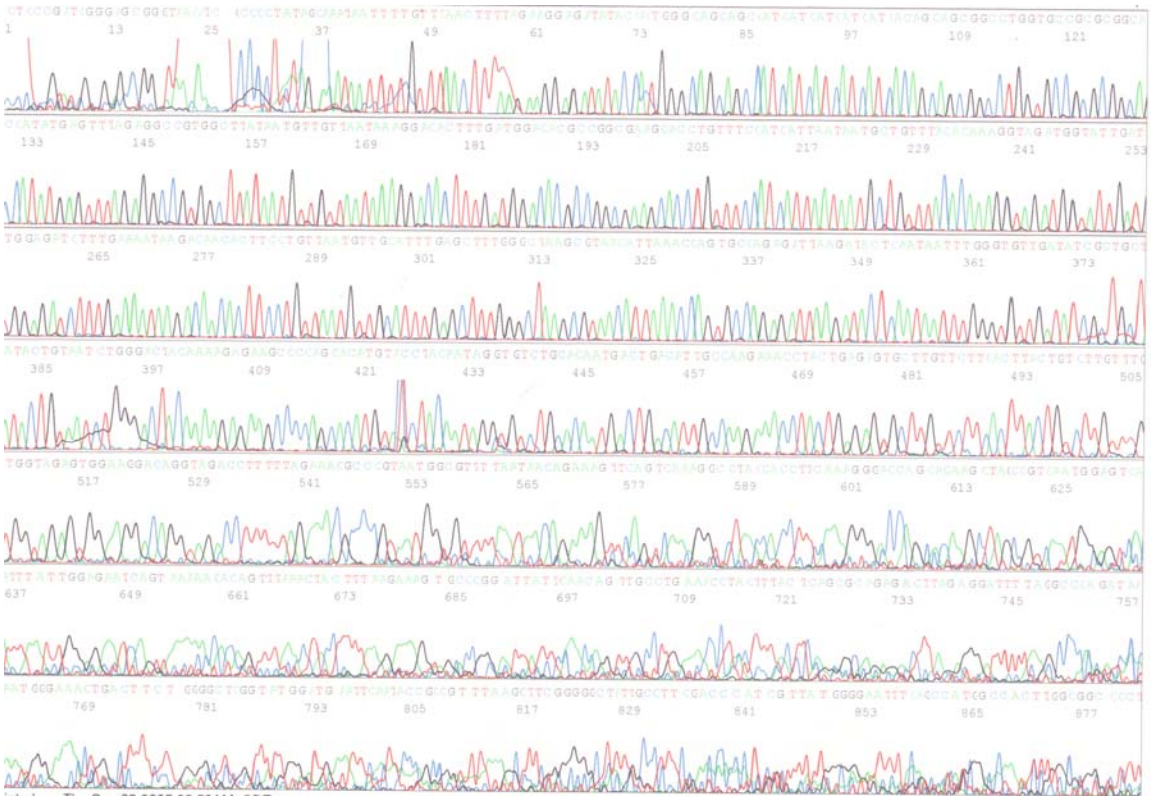

**Figure 3.4**: Nucleotide analysis of N4A promoter sequence. The nucleotide sequence was used to determine that the correct mutation had taken place, and no spontaneous mutations had occurred. The individual nucleotide bases can be seen below the curves.

As seen in Figure 3.4, each nucleotide in the DNA N4A terminator and promoter sequences was analyzed. The nucleotides corresponding with the correct mutations were then confirmed.

Analysis of Protein Expression assay for N4A and N4S

S cells containing T7 RNA polymerase were used in the transformation of the mutant DNA. T7 RNA polymerase was necessary in order to make the mutant protein. The S cells were the competent cells of choice due to their mutations in protease genes thereby decreasing degradation of expressed proteins. The protein was extracted and fractions from the Talon Nickel Affinity column were saved throughout the assay. The protein extraction gel for N4A and N4S can be seen in Figure 3.5.

Each lane shows protein that was eluted from the column. The final elutions, E1 and E2 contain the purified N4A and N4S. The total ($2^{nd}$ lane) contains large amounts of extraneous protein along with N4A and N4S. The load ($3^{rd}$ lane) shows the protein (including extraneous protein) that was added directly to the Talon-Nickel Affinity column. The flow through ($4^{th}$ lane) shows the extraneous protein that passed through the column via gravity filtration. The low concentration imidazole wash ($5^{th}$ lane—wash2) contains more extraneous protein that may have transiently bound to the column, along with other extraneous protein that was not removed in the flow through. N4A and N4S were bound to the Talon resin via histidine tags. In order to remove the desired protein from the column, higher concentration of imadazole was used. Imidazole contains histidine and removes N4A and N4S by eluting it from the column bound to the histidine. N4A and N4S are somewhat purified here, but not completely; a few extra bands are seen for extraneous proteins.

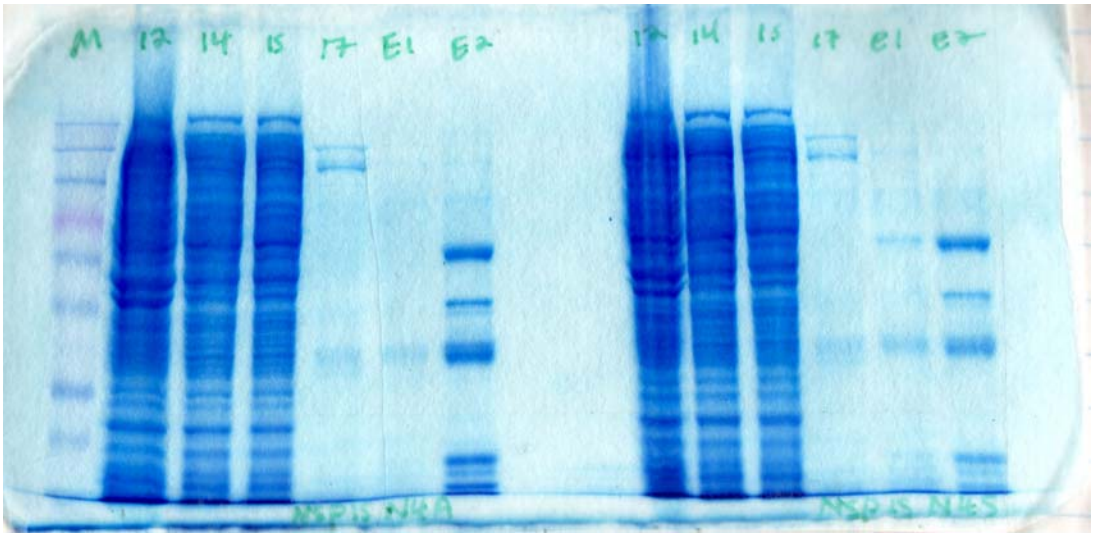


**1 2 3 4 5 6 7 8 9 10 11 12 13**

**Figure 3.5**: N4A and N4F protein extraction gel. N4A:1st lane = protein bench marker; 2nd lane = total protein; 3rd lane = supernatant loaded onto Talon column; 4th lane = flow through; 5th = low imadazole wash; 6th – 7th lanes = elutions of purified N4A. N4S: 8th lane = total protein; 9th = supernatant loaded onto column; 10th lane = flow through; 11th lane = low imadazole wash; 12th – 13th lanes = elutions of purified N4S.

FPLC Analysis

In order to further purify the protein, Fast Protein Liquid Chromatography was run. The MonoQ column used in FPLC separated the protein according to charge. Salt buffers were used during the filtration to affect the charge of the column, thus separating the protein at different fractions. The flow diagrams from the FPLC show the fractions in which the protein is contained (see Figure 3.6 for N4S; see Figure 3.7 for N4A). The pink and red lines on the diagram shows the points of injection for the high and low salt buffer solutions. The large, erratic recording shows an air bubble in the sample. The protein was found to be in fractions 24-30, as seen by the smooth curves at the right of

the diagram. (The last smooth curve was affected by the salt buffers, and does not contain protein).

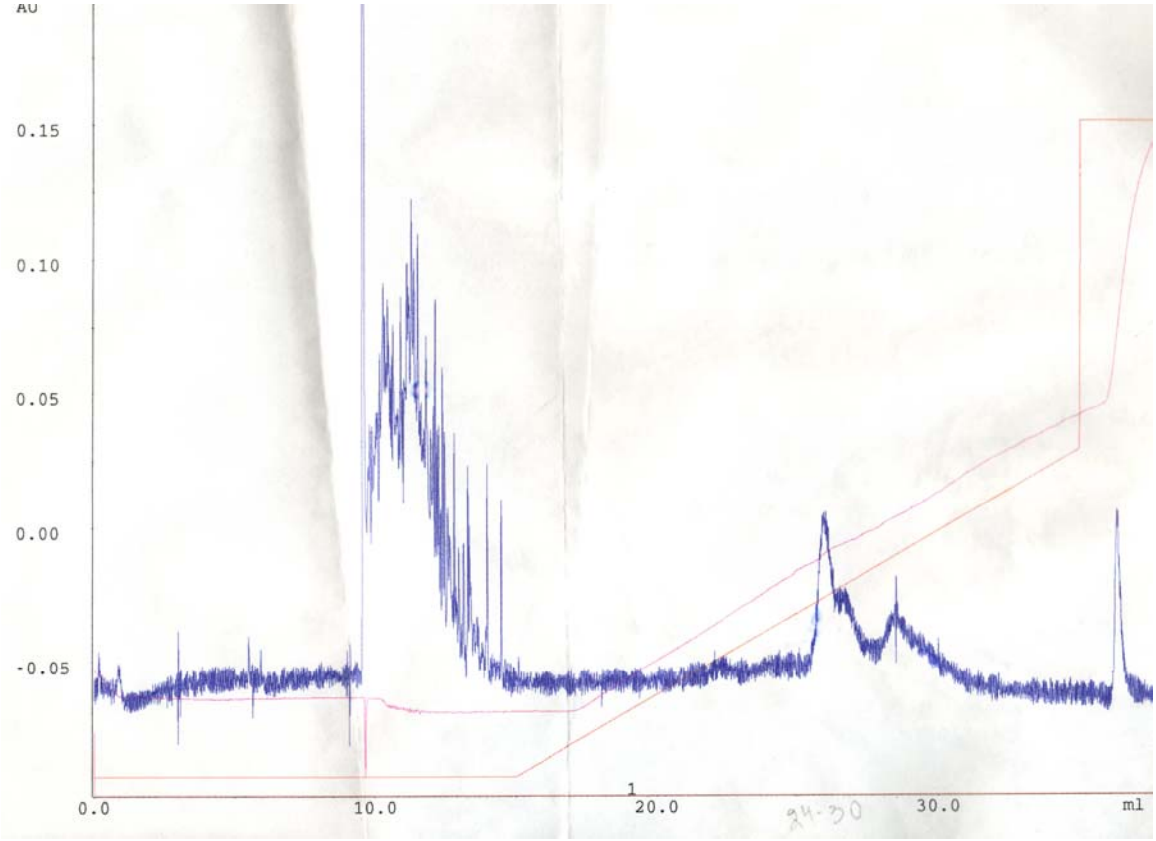


**Fractions:** **24** **30**

**Figure 3.6**: FPLC diagram for N4S. Protein can be seen in the smooth curves corresponding to fractions 24-30.

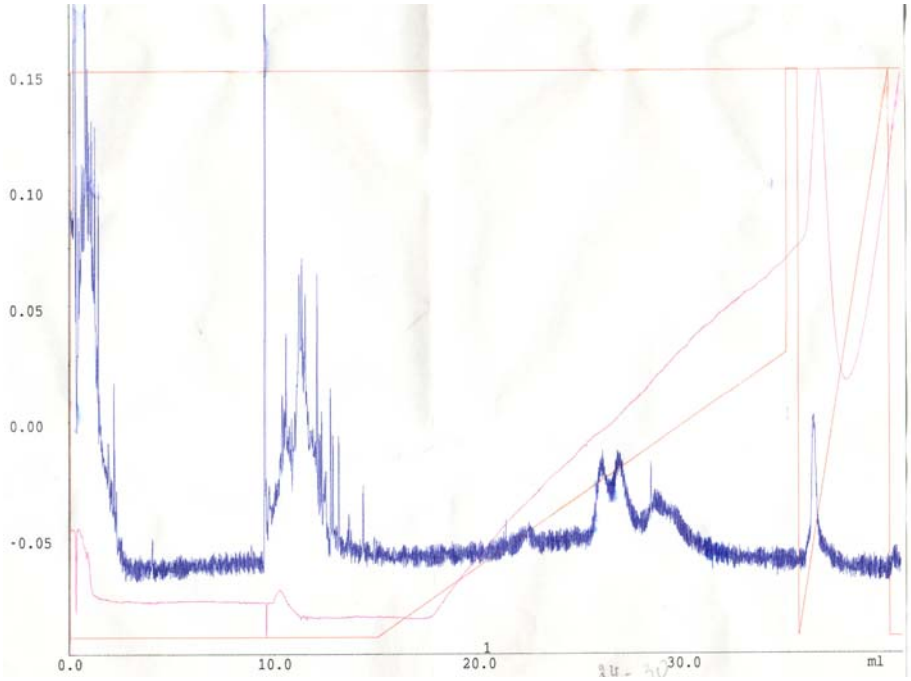


**Figure 3.7:** FPLC diagram for N4A; fractions 24-30 contained protein as modeled by the smooth curves labeled above.

The fractions with protein were run on a 10% SDS page gel, as seen in Figure 3.8. The fractions with the largest bands were combined, and used for further analyses as the sample for N4A and N4S.

Concentration Analysis

N4A and N4S were compared against the standard Bovine Serum Albumin (BSA); a 10% SDS page gel was run in order to analyze the intensities of each band (see Figure 3.9. As compared to BSA= 1 µg/ µL, N4A was found to be 0.083 µg/µL and N4S was found to be 0.071 µg/µL. N4F, another mutant protein sample, was found to be 0.4 µg/µL


**N4A** **N4S**

**Figure 3.8**: Fractions 24-30 collected from MonoQ FPLC analysis. The darkest bands were combined (separately for N4A and N4S) and dialyzed for storage.

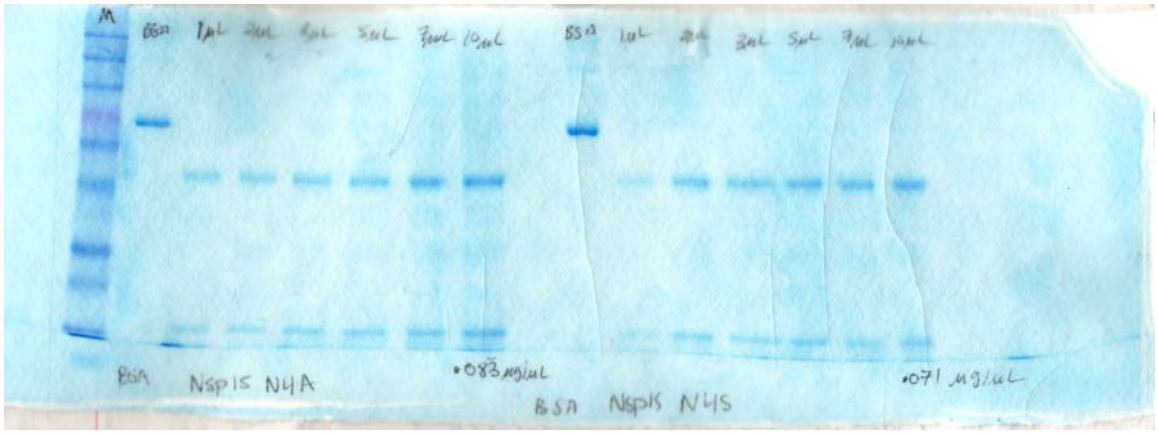


**1 2 3 4 5 6 7 8 9 10 11 12 13 14 15**

**Figure 3.9**: Concentration gel for N4A and N4S. <u>N4A:</u> 1st lane = protein bench marker; 2nd lane = BSA; 3rd lane = 1 µL; 4th lane = 2 µL; 5th lane = 3 µL; 6th lane = 5 µL; 7th lane = 7 µL; 8th lane = 10 µL; <u>N4S:</u> 9th lane = BSA; 10th lane = 1 µL; 11th= 2 µL; 12th lane = 3 µL; 13th lane = 5 µL; 14th lane = 7 µL; 15th lane = 10 µL.

A concentration gel was also run in order to compare all mutants (N4A, N4S and N4F) with the wild type (see Figure 3.10).

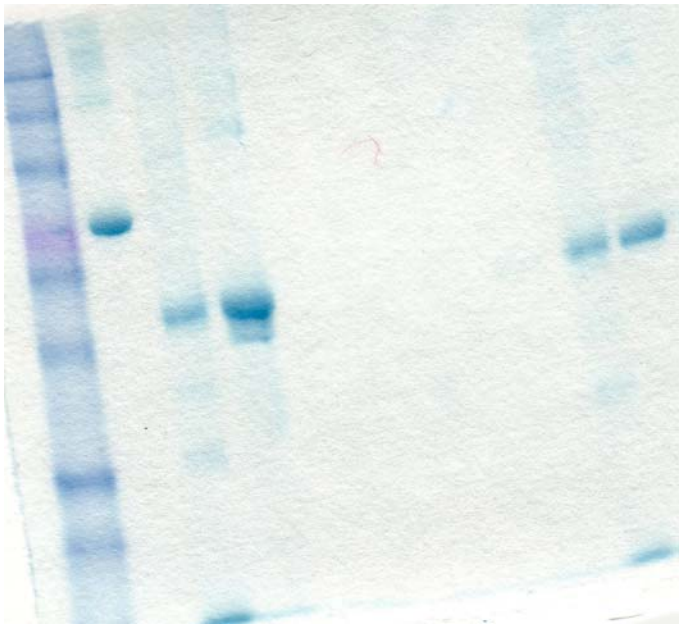

**1 2 3 4 5**

**Figure 3.10:** All mutants compared with wild type and BSA: (from left) Protein bench marker, BSA, N4A, N4S, N4F, and wild type.

A dilution series of N4F at 2µL, 4 µL, and 6 µL was carried out on a 10% SDS page gel as seen in Figure 3.11.

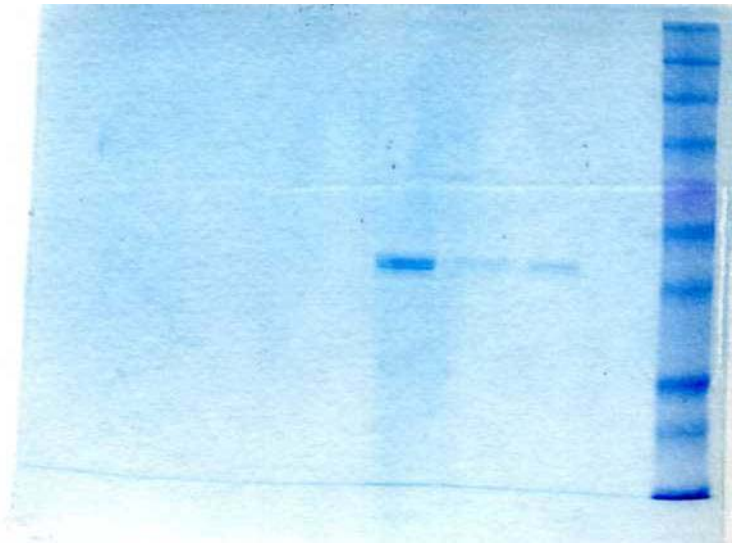

**1 2 3 4**

**Figure 3.11**: N4F in series with increasing concentration (from left) 6 µL, 4 µL, 2 µL, protein bench marker.

Activity Analysis

N4A, N4S, N4F, and wild type were run on a 28% Acrylamide-Urea gel, and radioactive RNA (marked with a radioactive isotope, $^{32}P$) was added. The gel was blotted onto a film, and imaged; the image was visible due to the radioactive isotope of phosphorous, $^{32}P$, which was used to label the RNA substrate (see Figure 3.12). If cleavage was attained, it could be inferred that the mutation did not affect the activity of the protein. If cleavage was not attained, it could also be inferred that the activity was affected, and further tests should be run.

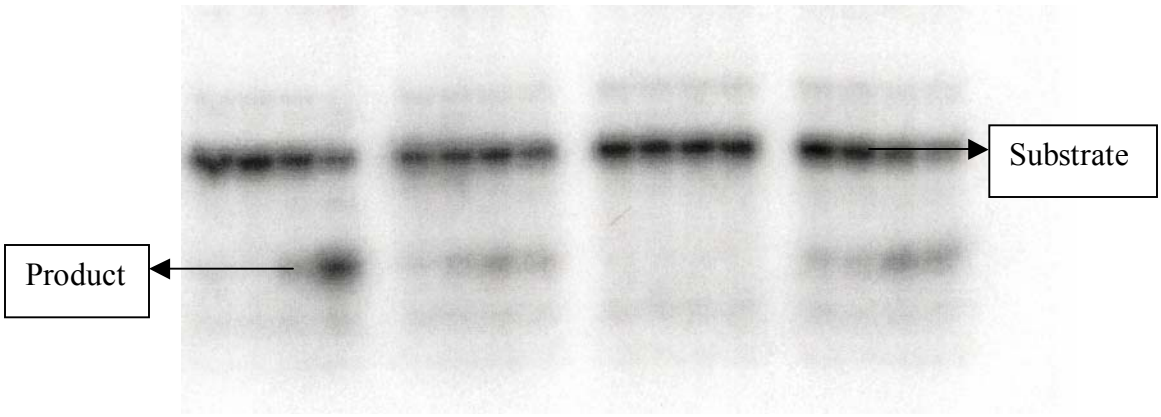


**Figure 3.12**: Phosphoimage yielding activity results: (from left) N4A, N4S, N4F, wild type

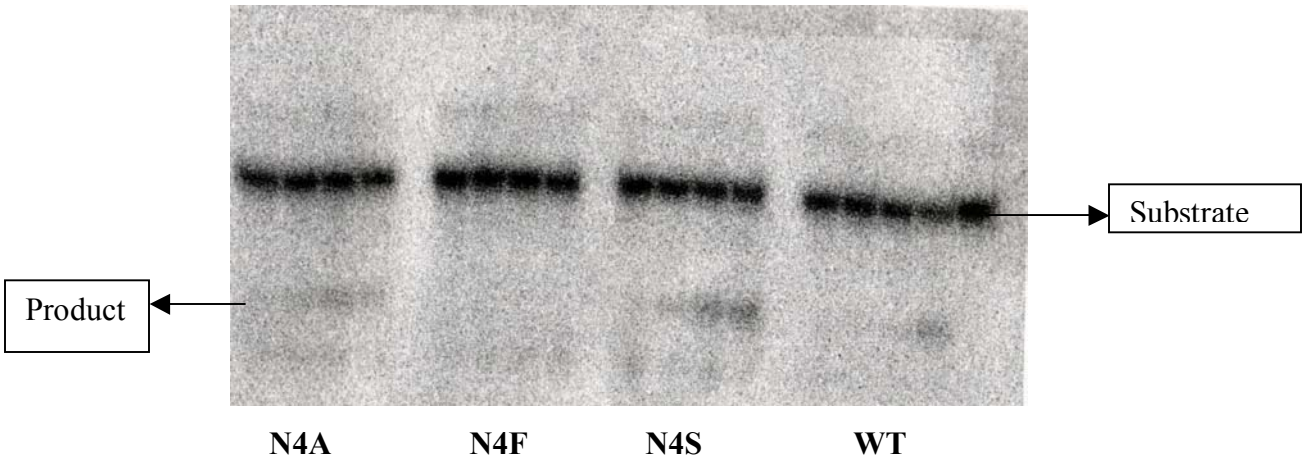


**Figure 3.13**: Phosphoimage obtained with old TRS probe: (from left) N4A, N4F, N4S, and Wild Type

The second bands in the above figure are the RNA cleavage products of Nsp 15 mutants and wild type. Results from the phosphoimage showed that N4A and N4S retained activity, whereas N4F did not. The TRS radioactive probe (radiolabeled RNA) should be fresh to attain best results. An old probe was used for one trial, and the image was unclear. The assay was run for a second time with a new TRS probe, and the image was clear, (see Figure 3.13 for fuzzy image obtained with old probe).

To better compare the wild type to N4F, a 28% acrylamide-urea gel was run. N4F and wild type were imaged together for better comparison (see Figure 3.14).

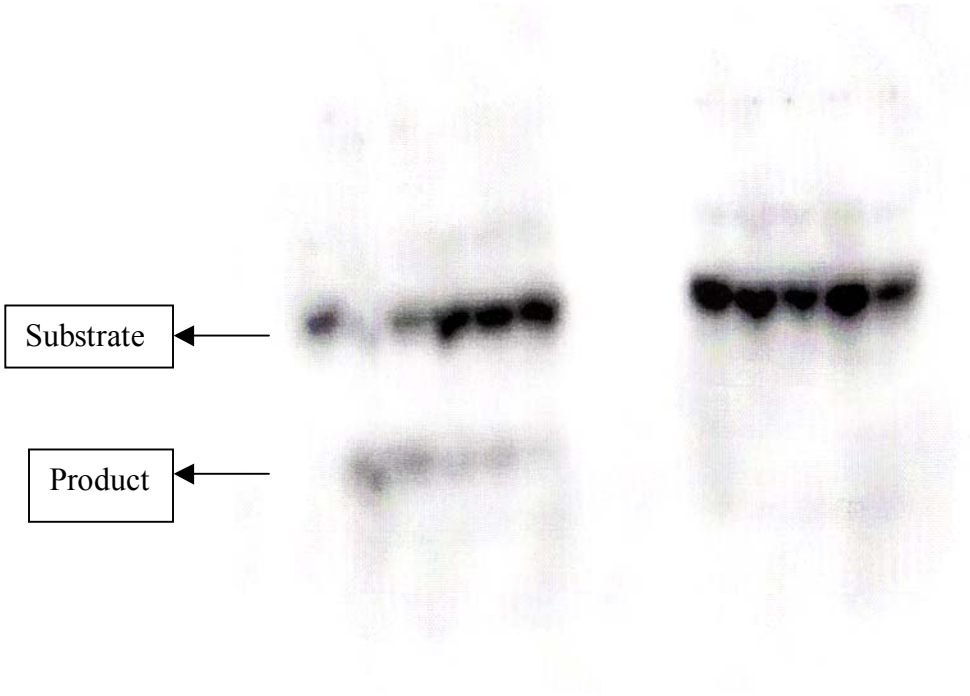


**Figure 3.14**: Phosphoimage of wild type and N4F. N4F has no cleavage product (2nd band), and therefore no activity

Since N4F had no activity in either phosphoimage, N4F DNA was transformed into S cells and the protein expression assay was repeated. It was found that N4F was not expressed; the protein seen in the gel (see Figure 3.15) was extraneous. The FPLC result showed no protein in any of the fractions (see Figure 3.16). After conducting a re-sequencing PCR, N4F was found to be mutated at positions other than the $4^{th}$ amino acid position. 2 other samples labeled N4S were thought to possibly be the true N4F. (It must be noted that the N4S that was created by site directed mutagenesis was truly N4S. N4S 1.87 and N4S 1.43 were two additional samples that were also labeled N4S). One of the samples had a concentration of 1.87μg/μL; the other had a concentration of 1.43μg/μL. Since the original sample thought to be N4F had a concentration of 1.87, it was thought that the true N4F also had this concentration. Both N4S 1.87 and N4S 1.43 were diluted to 0.25 μg/μL and a sequencing PCR was conducted. It was found that N4S 1.43 was truly N4F5G, and N4S 1.87 was also incorrect (figures not shown). None of the samples only had the N4F mutation.

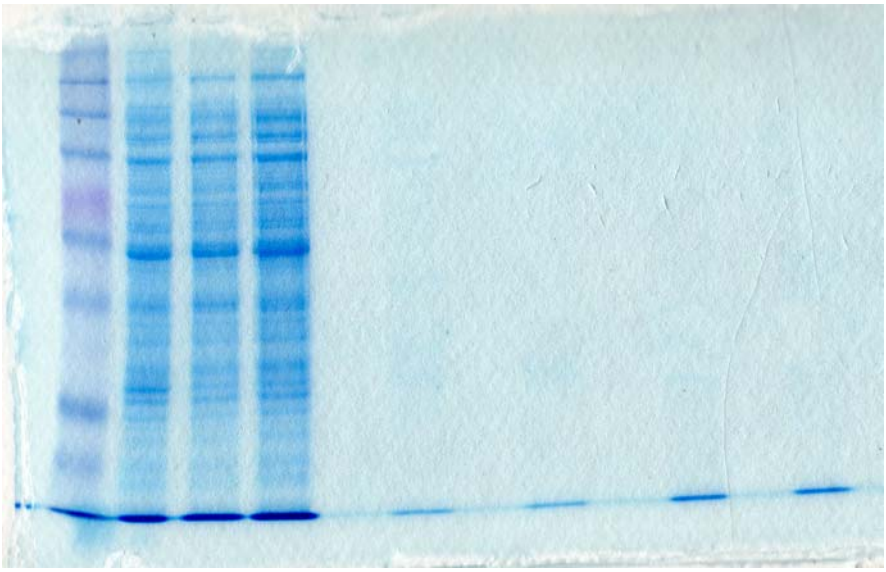

**1 2 3 4**

**Figure 3.15**: N4F: no protein in low imadazole wash or elutions. (Lanes with protein from the left) 1st lane = protein bench marker; 2nd lane = total protein; 3rd lane = supernatant loaded onto the column; 4th lane = flow through.

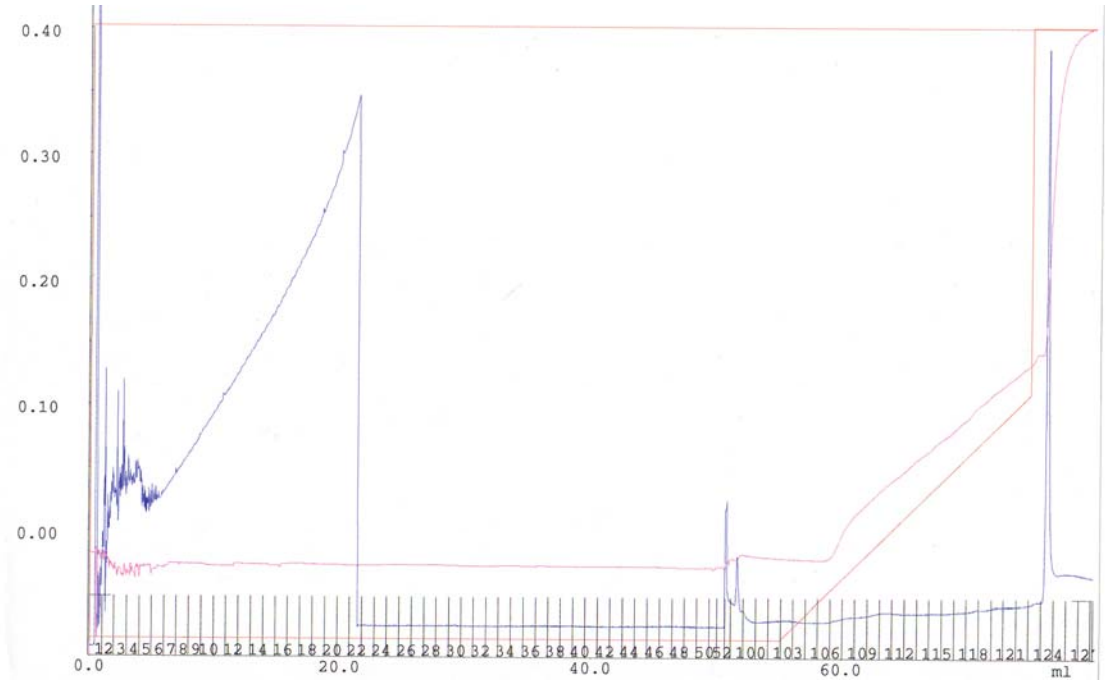


**Figure 3.16**: N4F FPLC; No protein was observed in the fractions from the FPLC

In order to make sure the N4F protein was not left in the pellet, thereby making it insoluble, the pellet was run on an extraction gel, along with the total, wash, and elutions. No protein was found to be in the pellet; this result confirmed the suspicion that N4F was not expressed (see Figure 3.17).

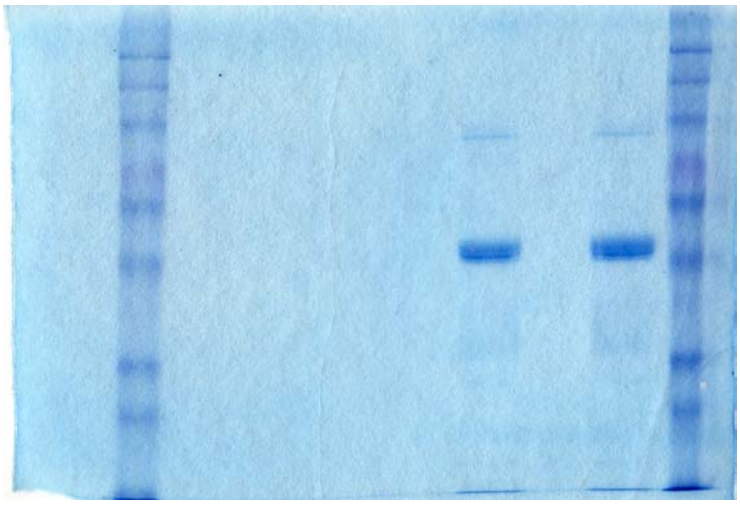

**1** **2** **gap** **3** **4**

**Figure 3.17**: No protein was found in the sample from the pellet (see gap between 2nd and 3rd lane)

Hexamer Formation Investigated

Gel filtration was implemented in the FPLC column Superdex 200 in order to test the hexamer and monomer formation of N4F in comparison with wild type. Gel filtration separated the proteins according to size. No hexamers were found in N4F and the monomer peak migrated differently than wild type monomers. This result would indicate that a subunit larger than a monomer, but smaller than a hexamer was obtained; this is impossible. Additional experimentation will be necessary to explore the structure of N4F (see Figure 3.18).

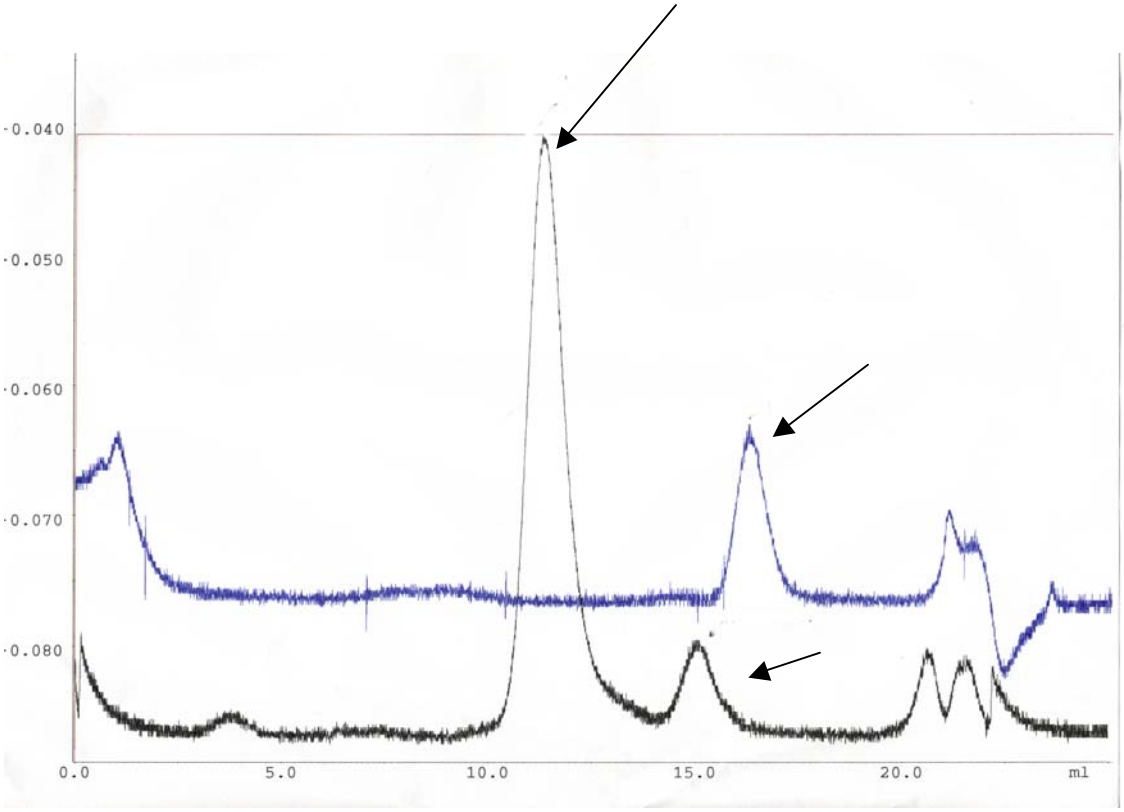


**Figure 3.18**: Conformations as found in fractions from FPLC. Top arrow points to the wild type hexamer peak; the shifted N4F peak is shown by the middle arrow. The bottom arrow shows the wild type and monomer peak. Equilibrium between monomers and hexamers is usual for wild type protein.

Discovery of N4F5G

N4F5G (formerly labeled N4S 1.43) was run on a 10% SDS page gel after protein extraction via a Talon-Nickel affinity column (see Figure 3.19).

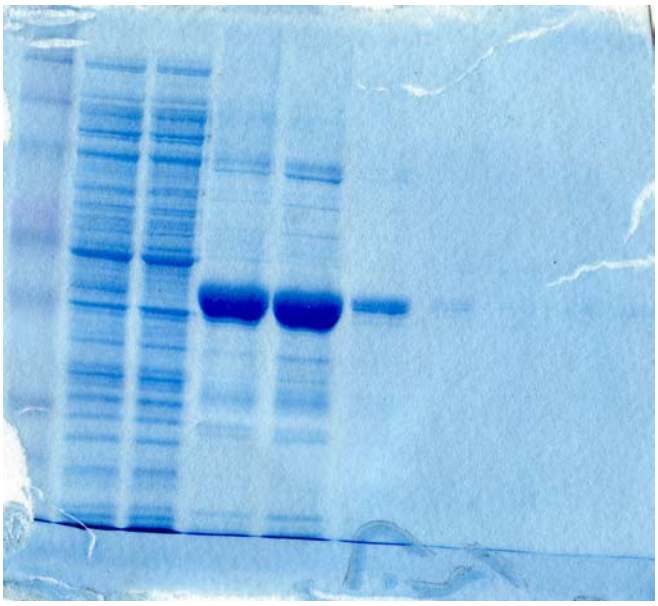

**L FT E1 E2 E3 E4**

**Figure 3.19**: N4F5G with protein in elutions: (from left) Load, flow through, elution 1, elution 2, elution 3, elution 4

Protein was found in the elutions from the Talon-Nickel affinity column indicating that the protein had in fact come off of the column, and was a soluble protein. N4F5G was tested with FPLC, and protein was found in the fractions (see Figure 3.20), as predicted by the gel in Figure 3.19.

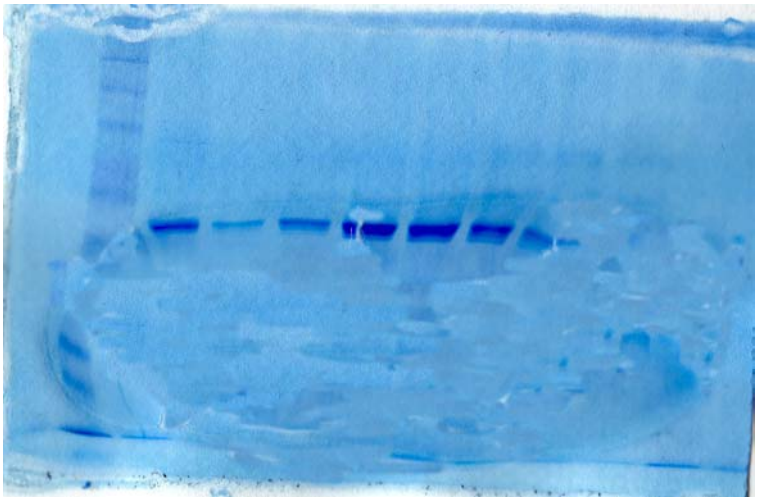

**Figure 3.20**: N4F5G protein seen in fractions from FPLC

Lys S Cells vs. S Cells

Lys S cells express lysosyme thereby helping to prevent expression of Nsp 15 prior to adding IPTG. S cells are deficient in RNase E. N4F5G was transformed into Lys S cells and S cells. Both cell lines were grown and the protein was extracted. In the 10% SDS page gel, the protein made from the Lys S cells was not in the elutions from the column resin (E1, E2, and E3), whereas the proteins grown in the S cells did appear in the elutions (see Figure 3.21).

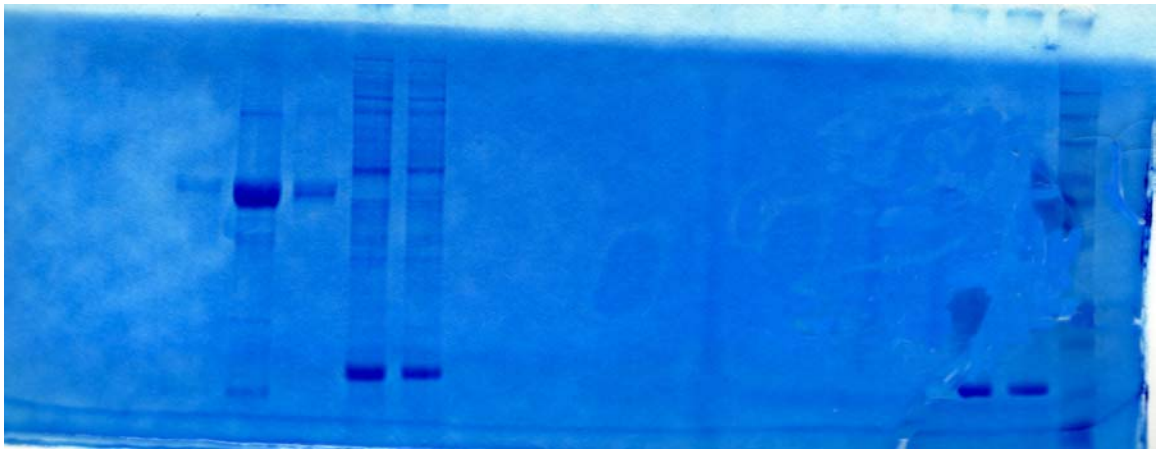

**S cells: 1 2 3 4 5 Lys S cells: 6 7 8**

**Figure 3.21**: N4F5G grown in S cells versus N4F5G grown in Lys S cells. There was no protein in the elutions from the Lys S cells. If there had been protein there would be bands before band 6 (from left).

# CHAPTER V
# SUGGESTIONS FOR FUTURE RESEARCH

For a more complete understanding of Nsp 15 endoribonuclease, more mutant proteins should be created, and the results quantified. By doing this, more information about the structure of the 4$^{th}$ amino acid position, along with other amino acid positions would be elucidated. With this information, more information can be gathered concerning the possible binding sites for the RNA substrate, and the amino acid sequences most responsible for the active 3D confirmation.

Further research should include testing the activity of N4F5G. In previous studies, E3A mutations in a similar ribonuclease caused conformational changes in the protein thereby affecting enzyme activity. With this in mind, mutating amino acids near the 3$^{rd}$ amino acid may result in changes in 3D conformation. If decreased or no activity is found, further experiments should be conducted to determine whether the activity change is due to an inability to bind the $Mn^{2+}$ cofactor, impaired RNA recognition, or to an inability to form hexamers.

In order to determine whether the mutant Nsp 15 bind $Mn^{2+}$, a titration experiment should be performed. Graphs of percent substrate cleaved vs. $Mn^{2+}$ concentration could then be constructed. The graphs would yield information on the binding affinity of the mutant for $Mn^{2+}$. From previous literature, it is hypothesized that the $Mn^{2+}$ cofactor induces a conformational change in Nsp 15, possibly to its catalytically active form. It is also recommended to test conformational changes produced by the

addition of $Mn^{2+}$ via intrinsic fluorescence (25). All mutant proteins would be compared to wild-type protein to look for abnormalities.

Mutant proteins could also be inactive because they fail to bind to the RNA substate. To test this possibility, fluorescence quenching could be used as the method to detect the bound RNA. The RNA substrate will be labeled with a fluorescent compound, and if Nsp15 binds to it, then the fluorescent signal will be decreased (25).

Lastly, conformational effects should be tested via native gel electrophoresis and gel filtration. Previous research has shown that Nsp15 forms a hexamer in solution (**Guarino**). Native Nsp 15 has a molecular weight of around 240,000 kDa, although the predicted molecular mass is only 40,000 kDa. This would help in adding to the literature on the active confirmation of Nsp 15. Once the active confirmation is better understood, more information can be gathered on how the protein functions in vivo with other proteins, thereby taking one step closer to understanding the viral mechanism for structure based drug design.

# CHAPTER IV
# CONCLUSION

By inserting various amino acid mutations into the Nsp 15 endoribonuclease, it was found that endoribonuclease activity was affected. N4F caused the endoribonuclease activity to cease. The N4A mutation as well as the N4S mutation retained activity. From this, it can be inferred that the N4F mutation caused severe hexamer disruption thereby ceasing endoribonuclease activity. It must also be noted that the N4F used in the activity assay was severely mutated in positions exceeding the 4$^{th}$ amino acid position. More research should be done with the F mutation only in the 4$^{th}$ amino acid position, (more detail on implications for future research can be found in Chapter V).

Knowledge of Nsp 15 endoribonuclease may one day lead to the discovery of structure based drugs used to treat SARS. The protocols followed in these experiments may be specific for Nsp 15, but the discovery process and pattern of thought necessary can be applied to all areas of scientific research. It was the goal of this research endeavor to add to the literature on Nsp 15 endoribonuclease by creating a better understanding of the structural and functional capabilities of Nsp 15, and how they can be manipulated for treatment.

# LITERATURE CITED


1. **Bartlam M., H. Yang, and Z. Rao.** 2005. Structural insights into SARS coronavirus proteins. Curr. Opin. Struct. Biol**. 15:**664-72.

2. **Bartlet, J.G.,** Johns Hopkins ABX Guide. 11 April 2006, accessed date. [Online.] http://hopkins-abxguide.org/show_pages.cfm?content=Jun-03_content.html

3. **Bhardwaj, K., L. Guarino, and C.C. Kao**. 2004. The Severe Acute Respiratory Syndrome Coronavirus Nsp15 Protein Is an Endoribonuclease That Prefers Manganese as a Cofactor. J. Virol. **78:**12218-12224

4. **Buchholz, U., A. Bukreyev, L. Yang, E. Lamirande, B. Murphy, K. Subbarao, and P. Collins.** 2004. Contributions of the structural proteins of severe acute respiratory syndrome Coronavirus to Protective Immunity. Proc. Natl. Acad. Sci. USA 2004. **101:**9804-9809.

5. **Chen L., C. Gui, X. Luo, Q. Yang, S. Gunther, E. Scandella, C. Drosten, D.Bai, X. He, B. Ludewig, J. Chen, H. Luo, Y. Yang, Y. Yang, J. Zou, V. Thiel, K. Chen, J. She, and H. Jiang.** 2005. Cinanserin Is an Inhibitor of the 3C-Like Proteinase of Severe Acute Respiratory Syndrome Coronavirus and Strongly Reduces Virus Replication In Vitro. J Virol. **79:**7095-7103.

6. **Dougherty, W.G., and B.L. Semler.** 1993. Expression of virus-encoded proteinases: functional and structural similarities with cellular enzymes. Microbiological Reviews **57:**781-822.

7. **Egloff, M., F. Ferron, V. Campanacci, S. Longhi, C. Rancurel, H. Dutartre, E. Snijder, A. E. Gorbalenya, C. Cambillu, and B. Canard.** 2004. The Severe Acute Respiratory Syndrome-coronavirus replicative protein Nsp9 is a single-stranded RNA-binding subunit unique in the RNA virus world. Proc. Natl. Acad. Sci. USA **101:**3792-3796.

8. **Garmen E.,** 2005. SARS proteomics reveals viral secrets. Structure (Camb) **13:**1582-1583.

9. **Graham, R.L., A. Sims, S. M. Brockway, R. S. Baric, and M. R. Denison.** 2005. The Nsp2 replicase proteins of Murine Hepatitus Birus and Severe Acute Respiratory Syndrome coronavirus are dispensable for viral replication. J. Virol. **79:**13399-13411.

10. **Groneberg, D.A., R. Hilgenfeld, and P. Zabel.** 2005. Molecular mechanisms of Severe Acute Respiratory syndrome (SARS). Respir. Res. **6:**8.

11. **Guarino, L.A., K. Bhardwaj, W. Dong, J. Sun, A. Holzenburg, and C.Kao.** 2005. Mutational analysis of the SARS virus Nsp15 endoribonuclease: identification of residues affecting hexamer formation. J Mol Biol. **353:**1106-17.

12. **Huang, Y., Z. Yang, W. Kong, and G. J. Nabel.** 2004. Generation of synthetic severe acute respiratory syndrome coronavirus pseudoparticles: implications for assembly and vaccine production. J. Virol. **78:**12557-12565.

13. **Holmes, K.,** 2003. SARS coronavirus: A new challenge for prevention and therapy. J. Clin. Invest. **111:**1605-1609.

14. **Ito, N., E. Mossel, K. Narayanan, V. Popov, C. Huang, T. Inoue, C. Peters, and S. Makino.** 2005. Severe Acute Respiratory Syndrome Coronavirus 3a Protein Is a Viral Structural Protein. J. Virol. **79:**3182-3186.

15. **Ivanov, K. A., T. Hertzig, M. Rozanov, S. Bayer, V. Thiel, A.E.Gorbalenya, and John Ziebuhr.** 2004. Major genetic marker of nindoviruses encodes a replicative endoribonuclease. Proc. Natl. Acad. Sci. **101:**12694-12699.

16. **Lau, S., P. Woo, K. Li, Y. Huang, H. Tsoi, B. Wong, S. Wong, S. Leung, K. Chan, and K. Yuen.** 2005. Severe acute respiratory syndrome coronavirus-like virus in Chinese horseshoe bats. Proc. Natl. Acad. Sci. USA **102:**14040-14045.

17. **Li Q., L.Wang, C. Dong, Y. Che, L.Jiang, L. Liu, H. Zhao, Y. Liao, Y. Sheng, S. Dong, and S.J. Ma.** 2005. The interaction of the SARS coronavirus non-structural protein 10 with the cellular oxido-reductase system causes an extensive cytopathic effect. Clin. Virol. **34:**133-9.

18. **Lin S., C.K. Lee, S.Y. Lee, C.L. Kao, C.W. Lin, A.B. Wang, S.M. Hsu, and L.S. Huang.** 2005. Surface ultrastructure of SARS coronavirus revealed by atomic force microscopy. Cell. Microbiol. **7:**1763-70.

19. **Lu J.H., Z.M. Guo, W.Y. Han, G.L. Wang, D.M. Zhang, Y.F. Wang, S.Y. Sun , Q.H. Yang, H.Y. Zheng, B.L. Wong, and N.S. Zhong.** 2005. Preparation and development of equine hyperimmune globulin F (abo) (2) against severe acute respiratory syndrome coronavirus. Acta. Pharmacol. Sin. **26:**1479-84.

20. **Marra, M.A., S. J. M. Jones, C.R. Astell, R. A. Holt, A. Brooks-Wilson, Y. S. N. Butterfield, J. Khattra, J. K. Asano, S. A. Barber, S. Y. Chan, A. Cloiytier, S. M. Coughlin, D. Freeman, N. Girn, O. L. Griffith, S. R. Leach, M. Mayo, H. McDonald, S. B. Montgomery, P. K. Pandoh, A. S. Petrescu, A. G. Rpbertson, J. E. Schein, A. Siddiqui, D.E. Smailus, J. M. Stott, G. S. Yang, F. Plummer, A. Andonov, H. Artsob, Nathalie, Bastien, K. Bernard, T. F. Booth, D. BOwness, M. Czub, M. Drebot, L. Fernando, R. Flick, M. Garbutt, M. Gray, A. Grolla, S. Jones, H. Feldmann, A. Meyers, A. Kabani, Y. Li, S. Normand, U. Stroher, G. A. Tipples, S. Tyler, R. Vogrig, D. Ward, B. Watson, R.C. Brunham, M. Krjden, M. Petric, D. M. Skowronski, C. Upton, R. L. Roper.** 2003. The genome sequence of the SARS-associate coronavirus. Science **300:**1399-1404.

21. **Numata, T., A. Suzuki, Y. Kakuta, K. Kimura, M. Yao, I. Tanaka, Y. Yoshida, T. Ueda, and M. Kimura.** 2003. Crystal structures of the ribonuclease MC1 mutants N71T and N71S in complex with 5'-GMP: structural basis for alterations in substrate specificity. Biochemistry. **42:**5270-8.

22. **Oehler, R.L.,** Severe Acute Respiratory Syndrome (SARS). 17 October 2005, accessed date. [Online.] http://www.emedicine.com/med/topic3662.htm

23. **Prentice E., J.McAuliffe, X. Lu, K. Subbarao, and M. Denison**. 2004. Identification and Characterization of Severe Acute Respiratory Syndrome Coronavirus Replicase Proteins. J Virol. **78**:9977–9986.

24. **Protein Engineering Glossary**. 11 April 2006, accessed date. [Online.] http://xray.bmc.uu.se/~kenth/bioinfo/glossary.html

25. **Ranjith-Kumar, C.T., Y.C. Kim, L. Gutshall, C. Silverman, S. Khandekkar, R.T.Sarisky, and C. C. Kao.** 2002. Mechanism of de novo initiation of RNA

synthesis by the hepatitius C virus RNA-dependent RNA polymerase: role of divalent metals. J. Virol. **76:**12513-12525.

26. **Rota, P. A., M. Oberste, S. Monroe, W. Nix, R. Campagnoli, J. Icenogle, S. Penaranda, B. Bankamp, K. Maher, M. Chen, S. Tong, A. Tamin, L. Lowe, M. Frace, J. DeRisi, W. Chen, D. Wang, D.D. Erdman, T.C. Peret, C. Burns, T. Ksiazek, P. Rollin, A. Sanchez, S. Liffick, B. Holloway, J. Limor, K. McCaustland, M. Olsen-Rasmussen, R. Fouchier, S. Gunther, A. Osterhaus, C. Drosten, M. Pallansch, L. Anderson, and W. Bellini.** 2003. Characterization of a novel coronavirus associated with severe acute respiratory syndrome. Science **300:**1394-1399.

27. **Snijder, E.J., P. J. Bredenbeek, J.C. Dobbe, V. Thiel, J. Ziebuhr, L. L. Poon, Y. Guan, M. Rozanov, W.J. Spaan, and A.E. Gorbalenya.** 2003. Unique and conserved features of genome and proteome of SARS-coronavirus, an early split-off from the coronavirus group 2 lineage. J. Mol. Biol. **331:**991-1004.

28. **Summary of probable SARS cases with onset of illness from 1 November 2002 to 31 July 2003.** 14 October 2005, accessed date. [Online.] http://www.who.int/csr/sars/country/table2004_04_21/en/

29. **Thiel, V., K. A. Ivanov, A. Puties, T. Hertzig, B. Schelle, S. Bayer, B. Weissbrich, E. J. Snijder, H/ Rabenau, H. W. Doerr, A. E. Gorbalenya, and J. Ziebihr.** 2003. Mechanisms and enzymes involved in SARS coronavirus genome expression. J. Gen. Virol. **84:**2305-2315.

30. **Wang X.W., J. Li, T. Guo, B. Zhen, Q. Kong, B. Yi, Z. Li, N. Song, M. Jin, W. Xiao, X. Zhu, C. Gu, J. Yin, W. Wei, W. Yao, C. Liu, J. Li, G. Ou, M. Wang, T. Fang, G. Wang, Y. Qiu, H. Wu, F. Chao, and J. Li.** 2005. Concentration and detection of SARS coronavirus in sewage from Xiao Tang Shan Hospital and the 309th Hospital of the Chinese People's Liberation Army. Water Sci. Technol. 52:213-21.

31. **World Health Organization**. 15 August 2002-7 August 2003. [Online.] http://www.who.int/csr/sars/country/en/country2003_08_15.pdf

32. **Yi C., L. Ba, L. Zhang, D. Ho, and Z. Chen.** 2005. Single Amino Acid Substitutions in the Severe Acute Respiratory Syndrome Coronavirus Spike

Glycoprotein Determine Viral Entry and Immunogenicity of a Major Neutralizing Domain. J Virol **79:**11638-11646.

**33. Zhang L., F. Zhang, W. Yu, T. He, J. Yu, C.E. Yi, L. Ba, W. Li, M. Farzan, Z. Chen, K.Y. Yuen, and D. J. Ho.** 2006. Antibody responses against SARS coronavirus are correlated with disease outcomes of infected individuals. J. Med. Virol. **78:**1-8.

**34. Ziebuhr, J. E., J. Snijder, and A.E. Gorbalenya.** 2002. Virus-encoded proteinases and proteolytic processing in the Nidovirales. J. Gen. Virol. **81:**853-879.

# CURRICULUM VITA

**Kimberlyn Maravet Baig**
2803 Camelot Drive, Bryan, Texas 77802
979-739-1641
maravet@neo.tamu.edu

## EDUCATION

*Brazos Christian School*
**High School Diploma** **May 2002**
Honors: Valedictorian, Physics Award 2002, Calculus Award 2002

Memberships: National Honor Society, Who's Who, Student Council

*Texas A&M University*
**B.S. in Molecular and Cell Biology** **December 2006**

Undergraduate Research Fellows Honors Thesis: "Site Directed Mutagenesis of the Severe Acute Respiratory Syndrome (SARS) Coronavirus Nsp 15 Endoribonuclease."
GPA: X.X

*Texas A&M University*
**B.S. in Biomedical Science** **December 2006**

Minor: Art and Architectural History
GPA: X.X

## HONORS AND AWARDS

- Biomedical Science Distinguished Student Award **2002**
- Dean's Honor Roll **2005-2006**
- Foundation Honors
- University Honors
- Undergraduate Research Fellows

## SCHOLARSHIPS

Valedictorian Award **2002**

Daniel W. Kempner Academic Excellence Award **2005-2006**

Julia Ball Lee Memorial Scholarship **2005-2006**

H.R. Lewis Memorial Scholarship **2005-2006**

Patricia A. Ward College of Medicine Scholarship **2006-2007**

## LEADERSHIP

*Aggie Women in Leadership*
Served as a junior mentor to underclassmen and attended various events involving women's role in leadership. **2003-Present**

*Texas A&M Pre-Medical Society: Community Service Chair*
Scheduled and Supervised community service activities for the executive team and society members. **2004-2005**

*Texas A&M Pre-Medical Society: President*
Governed the Texas A&M Pre-Medical Society both internally and externally. **2005-2006**

*Texas A&M Honor Council*
Served as Chair and as member of various Honor Council panels. Voted on the academic integrity of students as brought before the panel. **2004-Present**

## PAPERS AND RESEARCH

- "Hormone Effects on Carcinogenesis": investigated modern hormone replacement therapy via interview with Dr. Robin Fuchs-Young of MD Anderson Cancer Center.

- "Detection of Salmonellae in bovine feces by real time PCR." Sara D. Lawhon, G. Alex Klarenbeek, Roberta Pugh, Doris Hunter, William Miller, Carlos Rossetti, **Maravet Baig**, Andreas Bäumler, L. Garry Adams. (for publication)

- Conducted research in Dr. L. Garry Adams' lab 2004-2005

- Conducted research in Dr. Linda A. Guarino's lab 2005-2006 for Honors Undergraduate Research Fellows

## MEMBERSHIPS & HONOR SOCIETIES

- Texas A&M University Honor Council
- Phi Eta Sigma
- Sigma Xi
- Golden Key International Honour Society
- National Society of Collegiate Scholars
- Texas A&M Pre-Medical Society
- Aggie Women in Leadership